

**Stripe as an effective one-dimensional band of composite excitations**

A. L. Chernyshev\*

*Oak Ridge National Laboratory, P.O. Box 2008, Oak Ridge, Tennessee 37831*

S. R. White

*Department of Physics and Astronomy, University of California, Irvine, California 92697*

A. H. Castro Neto

*Department of Physics, Boston University, Boston, Massachusetts 02215*

(Received 25 January 2002; published 10 June 2002)

The microscopic structure of a charge stripe in an antiferromagnetic insulator is studied within the  $t$ - $J_z$  model using analytical and numerical approaches. We demonstrate that a stripe in an antiferromagnet should be viewed as a system of composite holon-spin-polaron excitations condensed at the self-induced antiphase domain wall (ADW) of the antiferromagnetic spins. The properties of such excitations are studied in detail with numerical and analytical results for various quantities being in very close agreement. A picture of the stripe as an effective one-dimensional (1D) band of such excitations is also in very good agreement with numerical data. These results emphasize the primary role of kinetic energy in favoring the stripe as a ground state. A comparative analysis suggests the effect of pairing and collective meandering on the energetics of the stripe formation to be secondary. The implications of this microscopic picture of fermions bound to the 1D antiferromagnetic ADW for the effective theories of the stripe phase in the cuprates are discussed.

DOI: 10.1103/PhysRevB.65.214527

PACS number(s): 74.20.Mn, 71.10.Fd, 71.10.Pm, 71.27.+a

**I. INTRODUCTION**

Strongly correlated models of the  $\text{CuO}_2$  planes of high- $T_c$  superconductors continue to attract much attention due to the belief that most of the physics in the cuprates is governed by strongly interacting, purely electronic degrees of freedom.<sup>1</sup> Microscopic studies of Hubbard and  $t$ - $J$  models have been successful in explaining the  $d$ -wave character of the pairing mechanism<sup>2-5</sup> and other experimental results, such as narrow low-energy bands in the angle-resolved photoemission for the undoped systems.<sup>6-8</sup> More recent interest in these models has been boosted by the discovery of stripes, or spin and charge inhomogeneities, in high- $T_c$  materials.<sup>9,10</sup> Generally, the strongly correlated  $t$ - $J$  and Hubbard models in the non-perturbative regime ( $J \ll t$  or  $U \gg t$ ) are difficult to approach analytically, although some advances have been achieved in solving them. Because of this, numerical methods have been responsible for much of the progress in the understanding of these models.<sup>11-14</sup> Moreover, such numerical studies have become a very important test of the ability of theoretical approaches to describe the stripe and other low-energy phases<sup>15</sup> in cuprates.

While the striped phase was anticipated from mean-field solutions of the Hubbard model,<sup>16</sup> probably the most convincing evidence of stripelike ground states has been provided by density-matrix renormalization group (DMRG) studies of the  $t$ - $J$  model in large clusters in the range of parameters relevant to real systems.<sup>17</sup> However, some other numerical approaches raise the question that the stripes seen in DMRG might be the result of finite-size effects.<sup>18</sup> Another aspect of the problem is that numerical studies alone do not directly answer questions on the origin of stripes. Ideally, one would wish for a theory which would closely agree with the numerical data on all essential aspects, thus providing a definite physical answer on how the stripes are created and

what are the excitations around this state. The search for such a case has motivated our present work and that is the way we unify our approaches here.<sup>19</sup>

In this work we attempt to integrate some of the earlier ideas on the  $t$ - $J$  model physics with the newer trends and phenomenology which have appeared due to stripes. We approach the problem using a comparative study of the stripe in an antiferromagnetic insulator by DMRG and an analytical technique, within the framework of the  $t$ - $J_z$  model. Our numerical study utilizes DMRG in large  $L_x \times L_y$  clusters of up to  $11 \times 8$  sites, using various boundary conditions. The analytical method is a self-consistent Green's-function technique developed earlier,<sup>20,21</sup> which accounts for the retraceable-path motion of the holes away from stripe. We demonstrate that the stripe in an antiferromagnet (AF) should be viewed as a system of composite holon-spin-polaron excitations condensed at the self-induced antiphase domain wall (ADW).

The  $t$ - $J$  model has long been seen as a natural model for the description of the charges and spins in a doped AF.<sup>22</sup> The single- and two-hole problems within the model have been studied extensively using different analytical schemes and numerical approaches in small clusters.<sup>11-14,23-32</sup> Some attempts to generalize the conclusions of these studies on the nature of the many-hole ground state have also been made.<sup>5,33-35</sup> Very good agreement between the numerical and analytical studies for these problems has been achieved within the spin-polaron paradigm.<sup>11,20,36,35</sup> This essentially quasiparticle picture describes the single-hole excitation as a hole strongly dressed by the "stringlike" spin excitations. It was found that two such quasiparticles tend to form a bound state of  $d$ -wave symmetry.<sup>11,24,29-32,37,38</sup> The generic reason for the absence of the  $s$ -wave pairing is the magnon-mediated exchange, which generates a repulsion in the  $s$ -wave channel.<sup>2,4,39</sup> In the  $t$ - $J$  model, vertex corrections are

suppressed<sup>23,40</sup> and such a repulsion is strong. Then the attraction in higher-order harmonics leads to the bound states of higher symmetry.<sup>41</sup> Attempts to integrate out the spin background and to reformulate the  $t$ - $J$  model as an effective model for quasiparticles with a narrow band ( $\sim 2J$ ) and an interaction repulsive in the  $s$ -wave channel and attractive in the  $d$ -wave channel have been made,<sup>5,34,35,38</sup> assuming the antiferromagnetic correlation length to be the largest scale in the problem. Phase separation in such a model in a physical range  $t \gg J$  seems to be unlikely since the pair-pair interaction should also be repulsive, which agrees with the numerical data.<sup>42</sup> The ground state in this model would be a dilute gas of  $d$ -wave spin-polaron pairs.

Such a generalization of the spin-polaron picture to a finite concentration of holes relies on the assumption that the antiferromagnetic background remains unchanged. However, it is well known that the feedback effect of holes on the antiferromagnetic background is important. Aside from Hartree-Fock treatments of the Hubbard model,<sup>16</sup> which showed stripelike domain-wall solutions, other studies of the  $t$ - $J$  model in the low-doping regime have indicated instabilities of the antiferromagnetic order.<sup>43</sup> These instabilities were thought to lead towards spiral,<sup>44</sup> stripelike spiral,<sup>45</sup> or spin-liquid<sup>46</sup> states. Earlier numerical works in the small  $t$ - $J$  clusters<sup>47</sup> have demonstrated stripes in the ground state which were also domain walls in the Néel AF. With the mounting evidence from experiments<sup>9,10</sup> and from DMRG numerical data<sup>17</sup> the idea of *topological* doping<sup>48</sup> has flourished. The spontaneously created ADW's have been widely considered as the topological alternatives to the homogeneous Néel background.<sup>49-52</sup>

Thus, the many-hole ground state has turned out to be very different from that for a few holes. In order to understand the nature of the charge excitations in this phase one needs to reconsider the single-particle problem around this ground state with different topology.<sup>53</sup> The one-dimensional (1D) character of the charge stripes has led to a number of attempts to generalize the physics of strictly 1D systems, where the excitations are holons and spinons, to higher dimensions.<sup>54,55</sup> On the other hand, there is a growing understanding that the stripes are the outcome of the same tendencies which are seen already for the single-hole problem,<sup>56</sup> and that the charge excitations in the stripe phase may still have lots in common with the spin polarons.<sup>21,57</sup>

Note that topological doping generally refers to the introduction of dopants into the topological defects of a field theory, which are the field configurations that interpolate between different vacua of the problem. For problems with high symmetry, such as the SU(2) Heisenberg model, topological defects are continuous distortions of the order parameter.<sup>58</sup> The ADW's are the topological defects for systems with lower  $Z_2$  symmetry, such as the Ising or the anisotropic  $t$ - $J_z$  model (and also models for polyacetylene<sup>59</sup>). While the magnetism in cuprates is very well described by the SU(2) symmetric models<sup>60</sup> the experimental finding of stripes indicate that topological doping corresponds to topological defects of lower symmetry. Although the reason for this lowering of the symmetry is, most probably, dynamical in nature and is still not clearly understood, it gives us con-

fidence that the  $t$ - $J_z$  model is the right starting point for the description of these systems.

As long as one is concerned with the short-range physics of the charge and spin excitations, the isotropic SU(2)  $t$ - $J$  and anisotropic  $t$ - $J_z$  models lead to similar results, as is well known from earlier studies.<sup>11</sup> Roughly, the hole motion is fast and the spin relaxation is slow when  $t \gg J$ . Therefore, in the fast time scale the hole moves in the background of essentially static, staggered spins. We will show below that the stripe phases obtained numerically for the  $t$ - $J_z$  model are virtually identical to those in the  $t$ - $J$  model studied before.<sup>17</sup> It has also been concluded, based on the Ginzburg-Landau functional approach, that the antiphase shift of the antiferromagnetic order parameter must originate from some short-range physics.<sup>61</sup> The rigidity of the  $\pi$  shift of the antiferromagnetic phase across the domain wall in both numerical and experimental studies also argues for the short-range genesis of the stripes.

In this paper we, therefore, study analytically and numerically the system of holes at the ADW in the anisotropic  $t$ - $J_z$  model. While we restrict ourselves to the study of the strongly anisotropic limit of the basic  $t$ - $J$  model, we believe that the results of our study are much more generic since the strongly correlated nature of the problem is preserved.

Technically, switching off the transverse spin fluctuation has numerical and analytical advantages. The numerical advantages are twofold. First, the sizes of the system which can be handled by the DMRG method are considerably bigger. Second, one can think of the boundary conditions as a way of stabilizing ground states of different symmetries. In our case the choice would be between the state with and the state without an ADW. Then, one can consequently dope holes in the stripe (ADW) configuration and study the evolution of the properties of the system as a function of doping, starting from a very dilute limit. It is worth noting the boundary conditions in our case work as a very gentle instrument of controlling the symmetry of the ground state *without* affecting the wave functions of the states themselves. The analytical advantage is the treatability of the problem. The analytical part of this work largely relies on a previous study by two of us and Bishop,<sup>21</sup> where we have calculated the Green's function of the charge excitation at the ADW by a method which goes beyond the limits of mean-field or perturbation theory.

The general conclusion of the present study is that the stripe should be considered as a collective bound state of the holes with an ADW. In such a system the excitations are composite holon-spin-polarons which populate an effective 1D band. This picture is in very good agreement with the numerical results and provides insight into the problem of the stripe phase in cuprates.

This paper is organized as follows. Section II describes various aspects of our analytical approach in detail. Section III describes the DMRG method. Section IV presents the results and comparison. Section V lists our conclusions.

## II. ANALYTICAL APPROACH

Our starting point is the  $t$ - $J_z$  model which is given by

$$\mathcal{H} = -t \sum_{\langle ij \rangle \sigma} (\tilde{c}_{i\sigma}^\dagger \tilde{c}_{j\sigma} + \text{H.c.}) + J \sum_{\langle ij \rangle} \left[ S_i^z S_j^z - \frac{1}{4} N_i N_j \right], \quad (1)$$

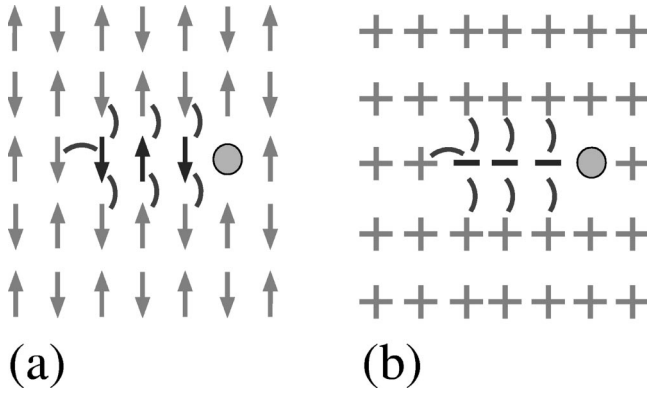


FIG. 1. (a) A hole followed by the string of spin defects in a homogeneous AF. (b) Same as (a), “+” and “-” denote the sign of the staggered magnetization  $M_i = (-1)^i S_i^z$ . Arcs denote wrong (ferromagnetic) bonds.

where  $t$  is the kinetic energy,  $J$  is the antiferromagnetic exchange, and  $N_i = n_{i\uparrow} + n_{i\downarrow}$ . All operators are defined in the space without double occupancy of the sites.

The single-hole problem for the  $t$ - $J$  ( $t$ - $J_z$ ) model in a homogeneous antiferromagnetic background is well studied with analytical results and numerical data being in very good agreement.<sup>11,20,35</sup> The charge quasiparticle is understood as a spin polaron, i.e., a hole dressed by strings of spin excitations.<sup>36</sup> It is also often expressed as that the hole movement in a homogeneous antiferromagnetic background is frustrated because of the tail of misaligned spins following the hole, see Fig. 1. The idea that an ADW can be a more favorable configuration for holes relies on the fact that such a frustration of the hole’s kinetic energy can be avoided for a movement inside the wall, such that the hole is essentially free in the 1D structure. However, as we show below, the spin-polaron aspect of the physics of the charge carrier remains very important in the stripe phase as well. We will first consider the specifics of the hole behavior in the inhomogeneous antiferromagnetic state (state with an ADW) and will address the spin-polaron aspect of the problem later. For the detailed description of the spin-polaron formalism used in this work we refer to Ref. 20.

### A. Holon in the domain wall

Since the stripe corresponds to an ADW in the spin background, one has to study the nature of charge excitations at such a domain wall. Let us consider the empty system first. The ground state is, of course, given by the simple Néel configuration of spins, Fig. 2(a). However, when the antiphase shift of the staggered magnetization is created (enforced by the boundary conditions, for instance) the straight bond-centered domain wall is the lowest energy state, Fig. 2(b). It has the energy  $E_{bond}^J = J/2$  per unit length, which is lower, for example, than the corresponding energy for the site-centered domain wall,  $E_{site}^J = 3J/4$ . We remark here that the SU(2) Heisenberg spins would prefer a continuous untwist from one end of the crystal to the other without a sharp domain wall.

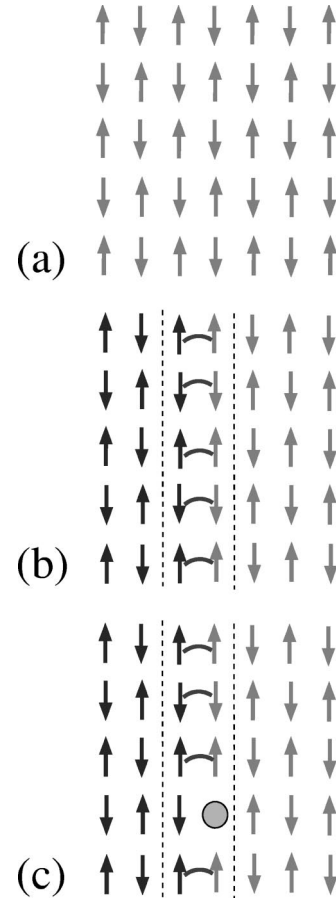


FIG. 2. (a) Homogeneous Néel state, (b) two domains of an AF with opposite staggered magnetization separated by the bond-centered ADW, (c) a static hole ( $t=0$ ) is attracted to the ADW. Arcs denote wrong (ferromagnetic) bonds.

Now let us consider a single hole doped to the system. When the kinetic energy is neglected ( $t=0$ ) the lowest-energy state is defined from simple bond counting. Evidently, the hole is attracted to the domain wall since the potential energy ( $J$  term) is lowered when the hole removes the wrong bond, Fig. 2(c).

When the kinetic energy is taken into consideration the following observation can be made. If one restricts the hole motion to one side of the ADW “ladder” of defects (along the  $y$  axes,  $x$  is fixed at  $x_0$  in Fig. 3) the problem is identical to the hole motion in the 1D Ising chain.<sup>62</sup> That is, one can see that after the first step, a 1D spin defect (spinon) is created and then the motion of the hole does not cause any further disturbance in the spin background, Figs. 3(a,b). The hole simply rearranges the wrong bonds while moving. Since the charge does not carry any memory about the spin of the place where it was created, this excitation is a holon. Notably, when the spinon and holon are separated, they both carry a kink or antikink of the staggered magnetic order; in other words, they are zero-dimensional ADW’s in the 1D chain problem, Fig. 4.

It is more visually convenient to use staggered magnetization  $M_i = (-1)^i S_i^z$  instead of the on-site magnetization to emphasize the opposite direction of the order parameter in

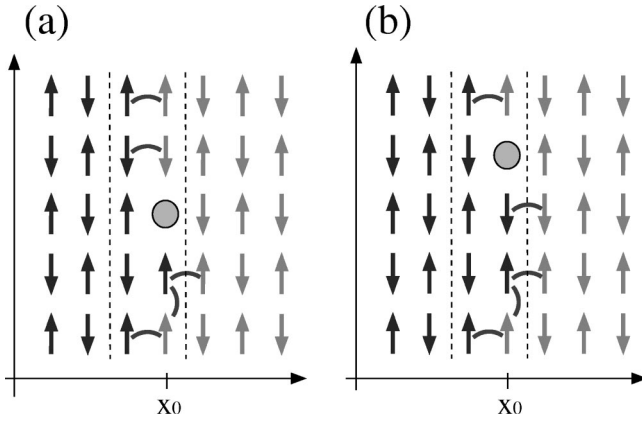


FIG. 3. Longitudinal hole motion along the ADW. The  $x=x_0$  line can be considered as an Ising chain. Arcs denote wrong (ferromagnetic) bonds.

the antiferromagnetic domains of spins. We, therefore, will often use “+” or “-” instead of the actual direction of the spin.

Since the spinon in our case is a finite-energy excitation ( $E_{spinon}=J/2$ ), in the  $t \ll J$  limit the hole will be always bound to its site of origin. One can think of several possibilities to avoid the spinon creation in order to focus on the properties of the charge excitation only. One can (i) assume that the crystal is finite (semifinite) and create a hole at one of the ends of the chain, then the propagation of the holon along the chain is free, (ii) create a pair of holes at the nearest-neighbor sites and then consider their motion independently, in this case both the kink and antikink are carried by holons, and (iii) start with the empty domain wall with a “wiggle,” one half of it misplaced by one lattice spacing from the other half along the  $x$  axis. This way one has an extra wrong bond in it, Fig. 5(a), which is equivalent to having a 1D chain along the  $x=x_0$  line with the single spinon. Then the hole creation at one of the sites forming the spinon is identical to the creation of a free holon, Figs. 5(b,c). The purpose of these manipulations is to show that the single-hole motion along the ADW can be made free provided that the spin environment ensures the holonic na-

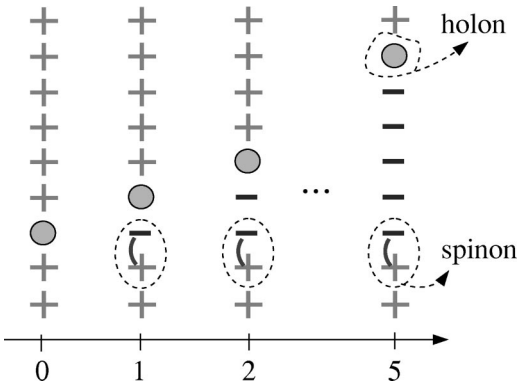


FIG. 4. Propagation of the hole in the Ising chain. Numbers indicate the amount of hoppings made by the hole away from its origin, “+” and “-” represent the sign of the staggered magnetization.

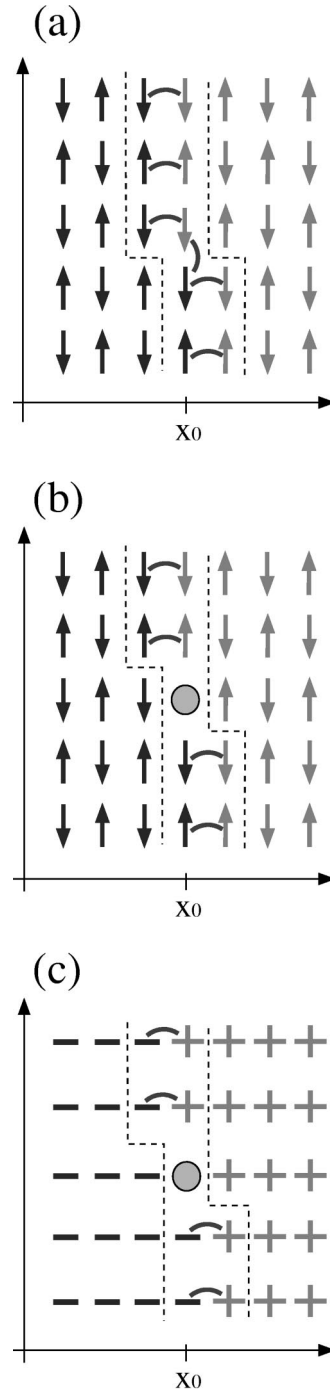


FIG. 5. (a) An empty ADW with the “wiggle.” For this configuration  $x=x_0$  line is an Ising chain with the single spinon. (b) A hole created at the place of the spinon is a holon. (c) Same as (b) with “+” and “-” showing the sign of the staggered magnetization. Arcs denote wrong (ferromagnetic) bonds.

ture of the charge excitation. These considerations are by no means new and were discussed in Refs. 63 and 64. We suggest calling the free motion of the hole within the stripe a “prepared-path” motion in accord with the “retraceable-path” motion for the spin polaron.

As it follows from the above consideration, the wave function of the single holon cannot be simply written as a

result of an action of a single annihilation operator on some unique ground-state wave function, since it requires a rearrangement of the (semi-) infinite amount of spins. However, if the ground state is “prepared,” as in the case (iii), one can still keep the formal similarity with the conventional single-particle creation. In other words, if the holon is to be created at the site  $i$ , its wave function can be written as

$$\begin{aligned}
 |1_i\rangle &= c_{i,\sigma_i} |\psi_{0,i}\rangle = (-1)^{i-1} \prod_{j<i} c_{j,\sigma_j}^\dagger \prod_{j>i} c_{j,\bar{\sigma}_j}^\dagger |0\rangle \\
 &\equiv (-1)^{i-1} |\dots \uparrow \downarrow \uparrow \downarrow \circ \uparrow \downarrow \uparrow \downarrow \dots\rangle \\
 &\equiv (-1)^{i-1} |\dots + + + + \circ - - - - \dots\rangle,
 \end{aligned} \tag{2}$$

where the Hilbert space at each site is restricted to single occupancy,  $\bar{\sigma} = -\sigma$ ,  $\sigma_j = \uparrow(\downarrow)$  if  $j \in A(B)$  sublattice,  $|0\rangle$  is the vacuum state, “+” and “-” denote the domains with staggered magnetization “up” and “down,” respectively. This definition suffices for our consideration.

The above-mentioned restriction of the hole motion along the ADW can be formally expressed as a separation of the kinetic-energy term in the Hamiltonian (1) in two pieces:

$$\mathcal{H}_t = \mathcal{H}_t^\parallel + \mathcal{H}_t^\perp, \tag{3}$$

where the first term (longitudinal) includes only 1D motion along  $y$  axis for  $x = x_0$  and the second term (transverse) includes the rest. Evidently,

$$\mathcal{H}_t^\parallel |1_i\rangle = t(|1_{i-1}\rangle + |1_{i+1}\rangle), \tag{4}$$

and thus

$$\mathcal{H}_t^\parallel |k\rangle = 2t \cos k |k\rangle, \tag{5}$$

where

$$|k\rangle = \sum_i e^{ikr_i} |1_i\rangle. \tag{6}$$

Consequently, the single-particle “bare” Green’s function of the free spinless fermion (holon) propagating along the ADW with simple tight-binding dispersion can be written as

$$G_{x_0}^{(0)}(k_y, \omega) = \langle k_y | \frac{1}{\omega - \mathcal{H}_t^\parallel} |k_y\rangle = \frac{1}{\omega - 2t \cos k_y + i0}, \tag{7}$$

where the zero of energy is set at the energy of the lowest static ( $t=0$ ) single-hole state  $E_0 = \langle \mathcal{H}_J \rangle_{t=0} = E_{I\text{sing}} + (L_y - 1)J/2 + 2J$ , and  $L_y$  is the size of the plane in the direction of the stripe. The holon band minimum is located at  $k_y = \pi$ , and the index  $x_0$  corresponds to the  $x$  coordinate of the stripe.

This observation that the hole can avoid the frustration of the antiferromagnetic background in the presence of an ADW in comparison with the homogeneous Néel state where the hole motion always leads to stringlike spin defects has been known since the discovery of the stripe phases. However, the sufficiency of this effect *alone* to justify the stripe formation has been exaggerated. Roughly speaking, this ar-

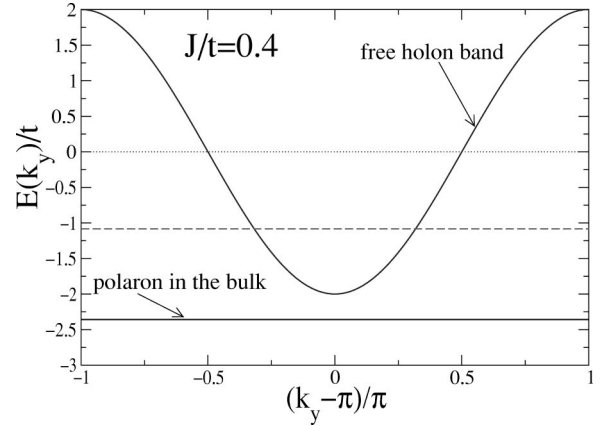


FIG. 6. The free-holon band ( $E_k = 2t \cos k$ , solid curve), energy of the spin polaron in the bulk (solid line), and energy per hole in the 1D holon band at half-filling,  $E_{1/2} = J/2 - 4/\pi$  (dashed line), are shown.

gument is gathered from the unphysical limit of the model,  $t \ll J$ , where the *kinetic* energy of the hole is indeed lower in the state with an ADW ( $E_{kin}^{ADW} \sim -t$ ) than in the homogeneous state with a spin polaron ( $E_{kin}^{sp} \sim -t^2/J$ ). However, the energy cost of the domain wall,  $E_{wall} \sim J$ , per unit length overwhelms this gain in kinetic energy in this limit. Moreover, the true ground state in the  $t \ll J$  limit is neither a stripe nor a homogeneous Néel state with holes, but rather the phase-separated hole-rich and no-hole states. In the physical limit  $t \gg J$  the “longitudinal” kinetic energy of the holon at the bottom of the ADW 1D band is  $-2t$ , while the energy of the hole (spin polaron) in the “bulk” (homogeneous Néel) is

$$E_{sp} = -2\sqrt{3}t + O(J^{2/3}t^{1/3}). \tag{8}$$

Evidently, the “unfrustrated” kinetic energy alone is insufficient to compete with the energy of the homogeneous state. We further illustrate this statement below.

Figure 6 shows the energies of the spin polaron in the bulk and the dispersion of the pure holon state at the ADW for the realistic ratio of  $J/t = 0.4$ . In the  $t$ - $J_z$  model the dispersion of spin polarons is small and we neglect it from this picture. One has to bear in mind that there is an (infinite) energy offset between these two lines: the energy of the ADW,  $E_J^{ADW} = L_y J/2$ . This simply means that the single holon cannot compensate the price for the domain-wall creation. Thus, the holon band must be filled to a certain level in order to reduce the energy. When we add more holes they will fill the higher  $k$  states in the band. Assuming a rigid-band filling the total energy per hole as a function of the 1D filling fraction  $n_\parallel$  can be calculated,

$$E_{tot}/N_h = \frac{J}{2} \left( \frac{1}{n_\parallel} - 1 \right) - \frac{2t \sin \pi n_\parallel}{\pi n_\parallel}. \tag{9}$$

which is infinite at  $n_\parallel \rightarrow 0$ ,  $E_{tot} = 0$  for completely filled band  $n_\parallel = 1$ , and has a shallow minimum at some intermediate value of  $n_\parallel$ . For a chosen value of  $J/t = 0.4$  this minimum is around  $n_\parallel^{min} = 0.32$ . This lowest energy  $E_{min} \approx -1.255t$  is a bit lower than the energy of the half-filled band  $E_{1/2} = J/2$

$-4t/\pi \simeq -1.07t$  shown in Fig. 6 by the dashed line. One can see that these energies are more than  $t$  higher than the energy of the spin-polaron system in the homogeneous Néel state  $E_{sp} \simeq -2.37t$ . Therefore, the energy balance of a narrow, strictly 1D stripe vs polarons is strongly against the stripe.

### B. Transverse hole motion

This illustration brings up the importance of the transverse part of the kinetic energy for the stripe formation. The transverse motion of a hole from the ADW, which includes all possible paths and not only those perpendicular to the stripe, is by no means different from the string type of propagation in the homogeneous AF, compare Figs. 1 and 7(a). That is to say that the charge excitation must essentially regain its spin-polaron properties away from the domain wall. Our Fig. 7(a) shows an example of a string generated by such a transverse movement. It is well known that the hole can propagate by erasing the tail of wrong spins via the so-called Trugman processes.<sup>65</sup> There is an important qualitative feature of our case which makes it different from the homogeneous problem in this aspect. Since the excitation inside the ADW is a holon, that is, the  $Q=1$ ,  $S^z=0$  excitation, while the spin polaron is a normal quasiparticle,  $Q=1$ ,  $S^z=\pm 1/2$ , the conservation of the quantum numbers requires the departure of the holon from the stripe to be always accompanied by the emission of the spinon ( $Q=0$ ,  $S^z=\pm 1/2$ ). This is clearly the case as is shown in Figs. 7(b,c).

In other words, the transverse hole motion should be considered as a decay process of the 1D (ADW) charge excitation into a 1D spin excitation and a bulk charge excitation, Fig. 8(a). Since both the holon dispersion and the holon-spin-polaron coupling are given by the same parameter  $t$  such virtual decays will lead to a strong renormalization of the holonic energy band.

As shown in Eq. (7) the bare Green's function of the hole residing at the ADW is the Green's function of a free spinless fermion (holon) with tight-binding dispersion. The renormalization of this Green's function is given by the self-energy schematically shown in Fig. 8(b). It is well known in the single-hole problem for the  $t$ - $J$  model that the self-consistent Born approximation, which is equivalent to the retraceable-path approximation in our case, accounts for the absolute majority of such a renormalization.<sup>20</sup> This latter fact is related to the effective analog of the Migdal theorem in this class of problems: all first-order corrections to the hole-magnon vertex are zero because of spin conservation.<sup>23</sup> Corrections from the higher-order processes, also known as Trugman paths,<sup>65</sup> remaining beyond the retraceable-path approximation are negligible. In anticipation of the further results we have to remark that in our problem the Trugman processes are simply forbidden by the conservation of quantum numbers for the holon decay. Therefore, the retraceable-path approximation should work even better due to the fact that the holon must emit the spinon with the energy  $\sim J$ . In other words, at least one spin excitation is always created and thus the Trugman paths belong to the same class as all other renormalization processes.

In our case the calculation of the self-energy in Fig. 8(b)

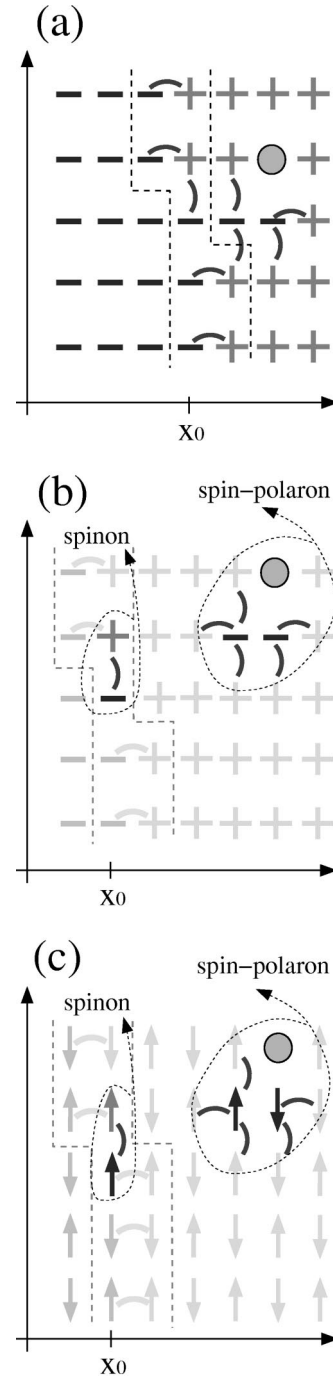


FIG. 7. (a) An example of a string generated by the transverse hole movement. Notably, the first defect in the string is a spinon in the  $x=x_0$  Ising chain. (b) A schematic result of the hole departure from the ADW, “+” and “-” showing the sign of the staggered magnetization as before. (c) Same as (b) with the actual spin directions shown.

is particularly simple since the spinon is a dispersionless excitation and the double line corresponds to the spin-polaron Green's function known from the previous studies.<sup>20</sup> As in the case of the spin polaron,<sup>20</sup> the renormalization is coming from the retraceable-path movements of the hole away from ADW and back. The full Green's function is then given by

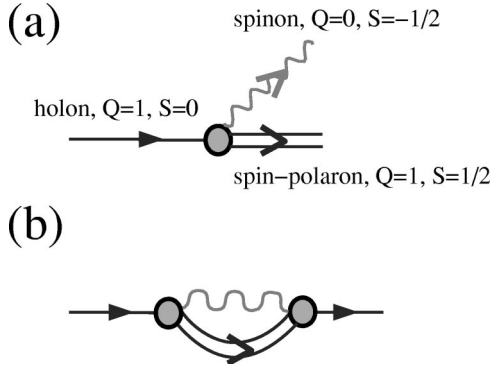


FIG. 8. (a) Decay of the holon into a spinon and a spin polaron. (b) The self-energy associated with such a decay.

$$G_{x_0}(k_y, \omega) = \frac{1}{\omega - 2t \cos k_y - \Sigma(\omega) + i0}, \quad (10)$$

where  $\Sigma(\omega)$  takes the form of a continued fraction,

$$\Sigma(\omega) = \frac{(z-2)t^2}{\omega - \omega_1 - \frac{(z-1)t^2}{\omega - \omega_1 - \omega_2 - \dots}}, \quad (11)$$

$z=4$  is the coordination number,  $\omega_i$  is the energy of the  $i$ th segment of the string, which is equal to the number of wrong bonds ( $J/2$  each) associated with the segment, index  $x_0$  corresponds to the  $x$  coordinate of the stripe.

The energy spectrum of the elementary excitations is given by the poles of the Green's function Eq. (10), therefore one needs to calculate  $\Sigma(\omega)$  and seek solutions of  $E(k_y) - 2t \cos k_y - \Sigma(E(k_y)) = 0$ . The resulting effective 1D band for the composite holon-spin-polaron excitation has been calculated in the previous work.<sup>21</sup> A standard simplification in the calculation of  $\Sigma(\omega)$  is to assume that all  $\omega_i$ 's in Eq. (11) are identical so that the energy of the string is simply proportional to the length of the path and is independent of the path of a hole. This is a good approximation for the spin polaron because only very few strings do not follow this rule. With this assumption the solution for the self-energy can be found in a compact analytical form given by the ratio of the Bessel functions.<sup>28</sup> If we take  $\omega_1 = J/2$  (energy of the spinon) and  $\omega_{i>1} = J$  [two wrong bonds per segment of the string, see Fig. 7(a)], the self-energy is<sup>20,28</sup>

$$\Sigma(\omega) = \frac{2t^2}{\omega - J/2 + \sqrt{3}tY(\omega - J/2)}, \quad (12)$$

with  $Y(\omega) = \mathcal{J}_{-\omega/J}(r) / \mathcal{J}_{-\omega/J-1}(r)$ ,  $\mathcal{J}_\nu(r)$  the Bessel function, and  $r = 2\sqrt{3}t/J$ .

For our problem this path-independent energy approximation also assumes that one can neglect the renormalization of the bulk spin-polaron wave function due to the vicinity of the ADW. However, there is a concern that this assumption may overestimate the energy of the excitation. Near the ADW there is less energy required to create a spin flip, therefore, there should be a subset of strings having a lower energy than the string of the same length in the bulk. That is, there is

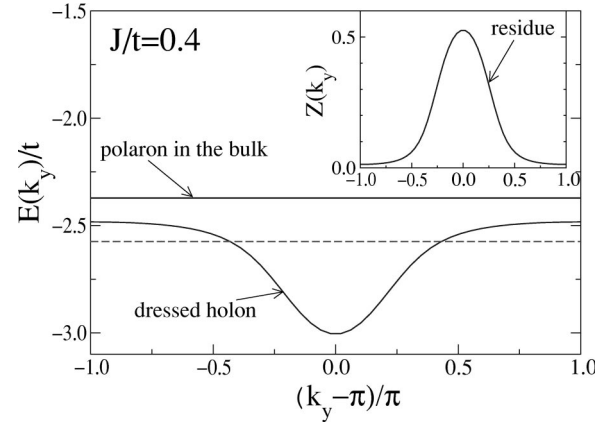


FIG. 9. Energy of an ADW elementary excitation  $E(k_y)$  vs  $k_y$  (solid curve). Solid straight line is the energy of the spin polaron in the bulk  $E^{sp}$ . These energies are relative to the energy of the static hole in a corresponding magnetic background, that is, the absolute energy of the ADW excitation is  $E_{wall} = (L_y - 1)J/2$  higher than that of the spin polaron. Dashed line is the total energy per hole in the half-filled 1D stripe band  $E_{1/2}$ , energy of the pure Ising state being subtracted. Since the reference energy for  $E_{1/2}$  and  $E^{sp}$  is the same, they can be compared directly. Inset: residue of the Green's function versus  $k_y$  (solid curves).

a question if the modification of the spin-polaron wave function is really negligible. While we will demonstrate below the adequacy of the above approximation, it can be shown that one can consider the problem more rigorously using the same approach by taking into account the energy of each string *exactly* up to a certain length  $l_c$  and applying the path-independent assumption only for  $l > l_c$ . Technically, it means that one can find all  $\omega_i$  in Eq. (11) up to some length of the string, use the explicit continued-fraction form of  $\Sigma(\omega)$  from Eq. (11) up to the same length  $l_c$ , and then use the approximate solution for the continued fraction  $\Sigma(\omega)$  from Eq. (12) for  $l > l_c$ . In other words, the modification of the spin-polaron wave function in the vicinity of the ADW can be consistently taken into account within the same approach.

The results of such calculations for a representative value  $J/t=0.4$  with  $l_c=4$  are shown in Fig. 9. The energy of the lowest pole of the Green's function versus  $k_y$  is shown by the solid line. As in Fig. 6 there is an infinite offset of the renormalized holon-spin-polaron band from the spin-polaron energy by the magnetic energy of the domain wall,  $E_{wall} = (L_y - 1)J/2$ . Since the effective band is significantly narrowed in comparison with the free band, the energy range shown in Fig. 9 is smaller than that in Fig. 6. One can see that the energy of the 1D ADW excitation with the energy of the magnetic background subtracted is now lower than the energy of the spin polaron in the bulk at all  $k_y$ , which means that the dressed 1D band is better for optimizing the kinetic energy than the homogeneous spin-polaron state.

Another informative quantity, the residue of the Green's function  $Z(k_y)$ , is shown in Fig. 9 (inset). It gives a measure of the amount of bare holon in the wave function of the elementary excitations. We avoid the use of the quasiparticle residue since the holon is not a quasiparticle in a strict sense, since its overlap with the physical electron is zero. However,

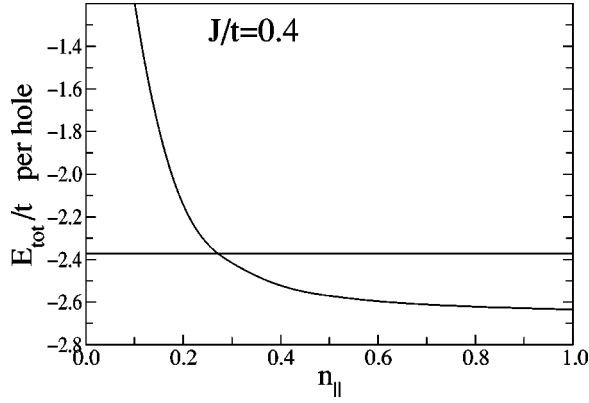


FIG. 10. Total energy of the system with ADW per hole versus 1D hole density  $n_{\parallel}$  (curve). Horizontal line is the total energy of free spin polarons in the homogeneous AF per hole. In both cases the energy of the pure Ising state is subtracted,  $J/t=0.4$ .

the residue preserves its original meaning, which refers to the renormalization of some bare excitation. One can see that a significant part of the initial holon at  $k_y = \pi$  resides inside the wall (about one half) and that almost all its weight is transferred to strings at  $|k_y - \pi| > \pi/2$ . Because the band is very flat at the same  $|k_y - \pi| > \pi/2$ , the velocity of the elementary excitations is much slower than the bare Fermi velocity  $v_F^0 = 2t \sin k_F / \hbar$ , in agreement with experimental findings.<sup>66</sup> It is easy to show that the velocity at the Fermi level for our 1D band is  $v_F = v_F^0 Z(k_F)$ . Generally, both the flatness of the top of the band and vanishing quasiparticle residue argue that the excitation at those  $k$  are only weakly attached to the stripe. The closeness of the bulk energy band to the top of the 1D stripe band suggests that the 1D excitations at the top of its band are not too different from the bulk spin polarons in the homogeneous AF.

### C. Stripe energy

For the chosen value of  $J/t=0.4$ , the energy of the holon at the bottom of the band is lower than the energy of the spin polaron by about  $1.5J$ , that is, the energy of three wrong bonds. Then the rough estimation gives that the magnetic energy of the domain wall will be compensated when in average every fourth site along the initial 1D chain is taken by the hole. That is, the kinetic energy will make the stripe to be the ground state at 1D linear hole concentration  $n_{\parallel} > n_{\parallel}^c \approx 1/4$  (for  $J/t=0.4$ ). A more accurate consideration should have the band-filling effects taken into account. Within the rigid-band approximation the total energy of the system per hole with the energy of the pure Ising state subtracted is

$$E_{tot}/N_h = \frac{J}{2} \left( \frac{1}{n_{\parallel}} - 1 \right) + \frac{1}{2\pi n_{\parallel}} \int_{\pi - k_F}^{\pi + k_F} E(k_y) dk_y, \quad (13)$$

where the first term is the domain-wall energy and the second term is the kinetic energy of the free quasiparticles filling the effective 1D band up to  $k_F = \pi n_{\parallel}$ . The total energy per hole of this 1D band indeed crosses the spin-polaron energy at around  $n_{\parallel} \approx 0.3$  as shown in Fig. 10. The total energy per hole at half-filling  $E_{1/2} \approx -2.57t$ , is shown in Fig. 9

by the dashed line. Above  $n_{\parallel} \approx 0.5$  the energy (13) versus  $n_{\parallel}$  is almost constant<sup>21</sup> with the energy difference between the stripe and no-stripe spin-polaron states of about  $-0.6J$ . This behavior of  $E_{tot}$  vs  $n_{\parallel}$ , the absolute value of the energy difference, as well as the value of  $n_{\parallel}^c$  are, of course, functions of the  $J/t$  ratio. However, these quantities only weakly depend on  $J/t$  in the realistic range  $0.1 < J/t < 0.5$  with  $n_{\parallel}^c$  shifting towards zero for smaller  $J/t$  (see also discussion of  $E_{tot}$  vs  $n_{\parallel}$  in Sec. IV).

An interesting question is what kind of energy scale defines the difference between a homogeneous state with spin polarons and a stripe state at some fixed  $n_{\parallel}$  (say  $n_{\parallel} = 1/2$ ),  $\Delta E = E^{sp} - E_{1/2}^{ADW}$ . By letting  $J/t \rightarrow 0$  we observe that  $\Delta E \rightarrow 0$  as well, and thus it cannot be proportional to  $t$ . This is in agreement with the expectation that at  $J=0$  all magnetic configurations should become degenerate. It is nevertheless hard to tell analytically or numerically if the leading term in  $\Delta E$  scales with  $J^{2/3}$  (however, see the discussion at the end of the section).

### D. Densities, electron distribution function

The knowledge of the single-particle Green's function not only allows us to calculate the energetic stability of the stripe as a function of  $n_{\parallel}$  and  $J/t$  (Ref. 21) but also enables us to find spatial profiles of the charge and spin densities,  $N(x)$  and  $|\langle S^z \rangle(x)|$ , as well as the electron distribution function  $n_{\mathbf{k}}$  for the stripe state.<sup>67</sup> To evaluate those quantities one needs to know the wave function of the 1D band excitation written in terms of the operators of spins and holes. If such a wave function is known for each  $k_y$  in the effective band then the distribution of the hole density and the damage of the spin density from the hole and strings can be extracted. Within the rigid-band picture these wave functions are orthogonal at different  $k_y$  and thus the density profiles are given by the superposition of the contributions from each  $k_y$ :

$$N(x) = \sum_{k_y < k_F} n^h(x, k_y),$$

$$|\langle S^z \rangle(x)| = \sum_{k_y < k_F} |\langle s^z \rangle(x, k_y)|, \quad (14)$$

where

$$n^h(x, k_y) = \langle \tilde{k}_y | \tilde{c}_j \tilde{c}_j^\dagger | \tilde{k}_y \rangle,$$

$$|\langle s^z \rangle(x, k_y)| = \langle \tilde{k}_y | \hat{S}_j^z | \tilde{k}_y \rangle, \quad (15)$$

where  $j=(x,y)$  and the choice of the  $y$  coordinate is arbitrary.

Such a wave function for our composite excitation can be written in a variety of ways. The simplest one is to write it as a linear combination of the components with strings of different length:<sup>24,25,37</sup>

$$|\tilde{k}_y \rangle = \sum_{l=0}^{\infty} C_{k_y, l} |l, k_y \rangle, \quad (16)$$

where  $|0, k_y \rangle$  is a pure holonic state and under the index  $l$  we also understand a summation over different paths of the same



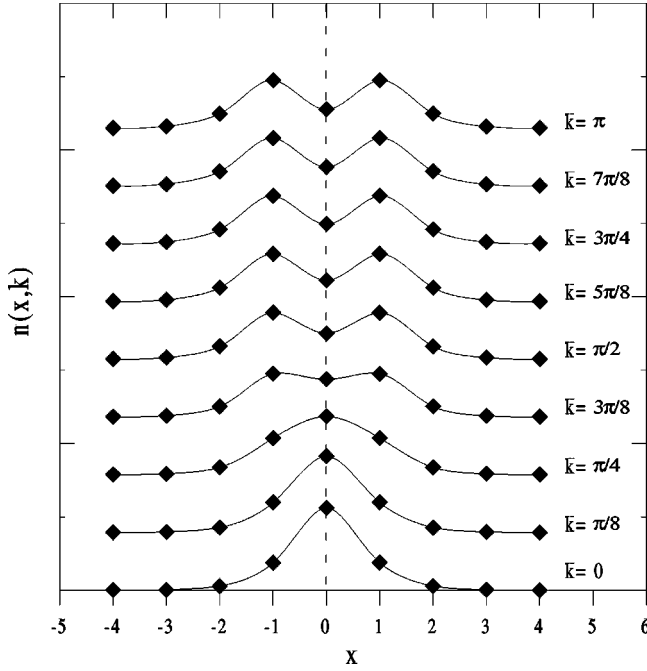


FIG. 11. The hole density modulation within the single-hole  $k_y$  eigenstate for different momenta  $k_y$ ,  $k = |k_y - \pi|$ . One can see that at the momenta away from the bottom of the band the hole is mostly spread around the stripe.

length  $l$ . Then, using a retracable-path approximation, it is easy to see that for each specific path

$$C_{k_y, l} = \frac{t \sqrt{Z_{k_y}}}{E_{k_y} - \omega_1 - \dots - \omega_l - \sum_{l+1} (E_{k_y})}, \quad (17)$$

where multiplier  $\sqrt{Z_{k_y}}$  comes from the normalization condition  $\langle \tilde{k}_y | \tilde{k}_y \rangle = 1$ . An equivalent expression for the spin-polaron case has been obtained in Refs. 27 and 28 using the spinless-fermion-Schwinger-boson representation for the original constrained fermion operators.

Since the hole density and the spin density are given by the averages of the local (on-site) operators their calculation using Eq. (16) is quite straightforward because they are diagonal in the string basis and do not provide transitions between different components of the wave function (16). Calculation of  $n_{\mathbf{k}}$  is technically more cumbersome since it is given by the nonlocal averages. One can always rewrite  $n_{\mathbf{k}}$  as

$$n_{\mathbf{k}} = \langle \tilde{c}_{\mathbf{k}}^\dagger \tilde{c}_{\mathbf{k}} \rangle = \frac{1}{N} \sum_i \left[ \langle \tilde{c}_i^\dagger \tilde{c}_i \rangle + \sum_{\mathbf{d} \neq 0} e^{i\mathbf{k} \cdot \mathbf{d}} \langle \tilde{c}_i^\dagger \tilde{c}_{i+\mathbf{d}} \rangle \right], \quad (18)$$

where we drop the spin index for clarity. One can see that the matrix elements between different strings are essential. For the details of calculations of  $n_{\mathbf{k}}$  in the  $t$ - $J$  model we refer to earlier works, Refs. 35, 68, and 69.

As an example of the calculation of the discussed quantities we show our results for  $n^h(x, k_y)$ , Eq. (15), in Fig. 11 for  $J/t = 0.4$ . This quantity shows the hole density modulation in the direction perpendicular to the stripe within the  $k_y$  eigenstate in the 1D band for different momenta  $k_y$ . One can see

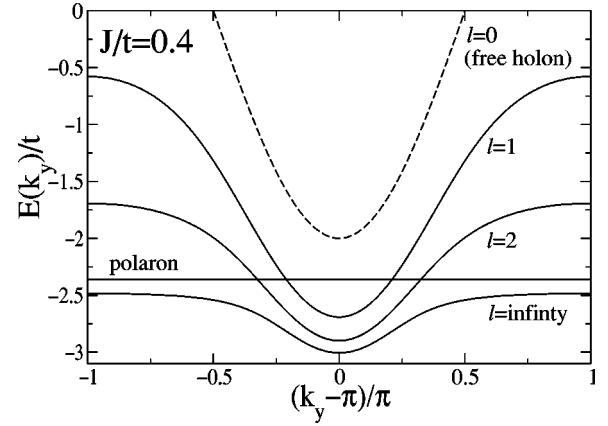


FIG. 12. Energy of an ADW elementary excitation  $E(k_y)$  vs  $k_y$  for strings with  $l=0, 1, 2, \dots, \infty$  included in the wave function.

that at the momenta away from the bottom of the band the hole is mostly spread around the stripe. Further results on these and other quantities are given in the context of the comparison with the numerical data, Sec. IV.

### E. Other questions

There are few other issues we would like to address here. First, if one is to start from the strictly 1D stripe and is to gradually relax the initial restriction for the hole to be kept in such a 1D chain, how soon does one reach the true eigenvalue of the  $t$ - $J_z$  Hamiltonian? That is, let us allow the bare holon to have an admixture of strings of length  $l=1, 2, \dots$  and see when the results converge and become independent of  $l$ . Figure 12 shows the energy bands for such restricted-string-length problems.  $l=0$  corresponds to a free holon, Fig. 6,  $l=1$  and  $l=2$  are for the cases where the strings of length 1 and 2 are included in the approximation.  $l=\infty$  is our answer from Eqs. (10)–(12), Fig. 9.

This comparison demonstrates one more time that the bare, or almost bare, 1D excitation with some admixture of the transverse fluctuations is certainly not a good approximation for the description of the stripe charge excitation. It is especially true for the finite concentrations where large momenta around  $k_F^{1D} \simeq \pi/2$  are most important.

As an alternative starting approximation we argue, once again, for the picture of a holon strongly coupled to the bulk spin-polaron excitation, Fig. 8. The dispersion obtained without renormalization of the spin-polaron propagator in Fig. 8(b) is shown by the dashed line in Fig. 13, which is already very close to the result where such a renormalization is taken into account (solid line, from Fig. 9).<sup>70</sup>

The second issue is the following. Since there are two types of kinks in the system (kink and antikink) which can be associated with the pure holonic excitation, Fig. 4, one can have two different species of excitations having opposite geometrical quantum numbers.<sup>63</sup> One may then think of them as essentially independent particles populating (quasi-) independent bands.

A little thinking brings such a logic into a paradox: the case when the chain is completely filled (all sites are occupied by holes) in this language will correspond to two half-

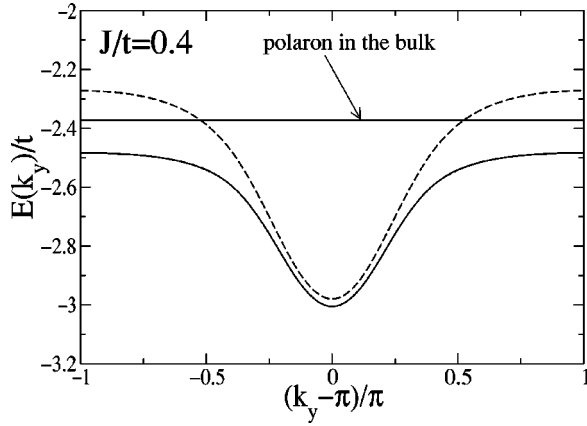


FIG. 13. 1D energy band for the composite excitation. Renormalization of the spin-polaron propagator at the vicinity of the ADW is included (solid line), not included (dashed line).

filled (conducting?) bands of different flavor. One resolves the paradox by noting that these extra quantum numbers should not lead to the increase of the total number of states in the system. In our case there cannot be more than one hole at any site while the assumption of independence of opposite species implicitly doubles the Hilbert space. Therefore, if one wants to keep two flavors in the problem, an infinite on-site repulsion between them should be introduced. That latter problem in one dimension maps exactly onto the problem of spinless, single-flavor particles<sup>71</sup> and thus the single-band approach used throughout this work is justified. Note that in the presence of the 2D degrees of freedom where the stripe as a whole can make wiggles, the problem of these geometrical quantum numbers becomes more complicated.<sup>63</sup>

The last question is what energy scale defines the free kinetic-energy difference between the stripe and no-stripe states. Naively, such  $\Delta E$  should be governed by the kinetic  $t$  term since the hole motion can be made free in a 1D structure. However, the energy of the order  $\sim JL$  is paid to prepare such a structure in a 2D AF. Let us consider the  $t \gg J$  limit for the 1D hole motion and assume that the length of the ADW is a free parameter which would minimize the total energy. In the continuum limit  $\langle E_{kin} \rangle = -2t + At/L^2$ ,  $\langle E_J \rangle$

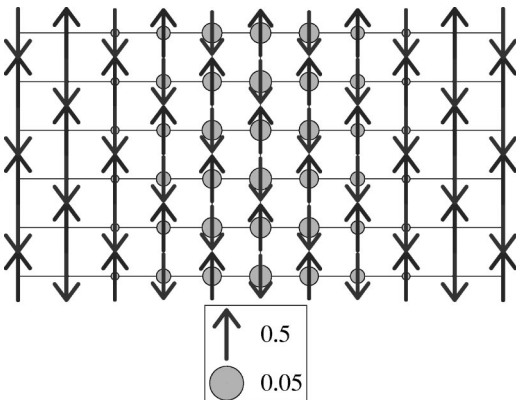


FIG. 14.  $11 \times 6$  cluster with one hole, cylindrical BC's, and  $J/t = 0.35$ . The size of the circles is proportional to the on-site hole density.

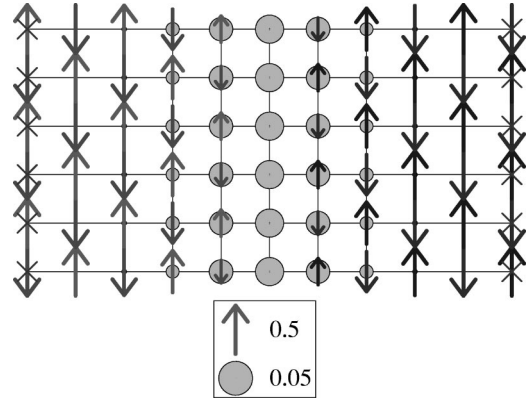


FIG. 15.  $11 \times 6$  cluster with one hole, field applied at open ends (crosses) to stabilize ADW,  $J/t = 0.35$ .

$\sim JL$ , and the minimum of the energy is achieved at  $L_{optimal} \sim (J/t)^{1/3}$ . The corresponding energy is  $E_{min} \approx -2t + \alpha(J^2t)^{1/3}$ . One recalls an almost identical consideration of the retracable-path motion of the hole by the strings in the spin-polaron problem which also gives  $\langle L_{string} \rangle \sim (J/t)^{1/3}$  and  $E_{sp} \approx 2\sqrt{3}t + \beta(J^2t)^{1/3}$ , see Ref. 36. Therefore, there is no new energy scale, different from the homogeneous Néel problem, introduced by the domain wall, and the prepared-path motion in 1D ADW is, in fact, not too different from the retracable-path motion of the hole within the spin polaron. One may conclude that the same scale  $\sim (J^2t)^{1/3}$  should govern the energetic balance favoring the stripe.<sup>72</sup> This is yet another argument that the stripes are the outcome of the same tendencies which are seen already for the single-hole problem.

### III. NUMERICAL APPROACH

The numerical study of the  $t-J_z$  model utilizes the DMRG method for the clusters up to  $11 \times 8$  with various boundary conditions (BC's). The BC's at the left and right sides are always open; if the BC's at the top and bottom are periodic we refer to the BC's as cylindrical. A staggered magnetic field, typically of size  $0.1t$ , can be applied at the open ends in order to enforce the ADW inside the system, or enforce it to stay homogeneous. Typically we keep 1000–2000 states per block, and perform up to a dozen finite system sweeps. Typically the truncation error was  $5 \times 10^{-5}$ .

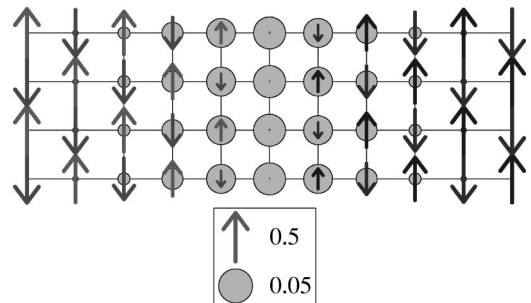


FIG. 16.  $11 \times 4$  cluster, one hole, open BC's in the narrow direction, no staggered field, cylindrical BC's,  $J/t = 0.2$ . The ground state here contains a stripe.

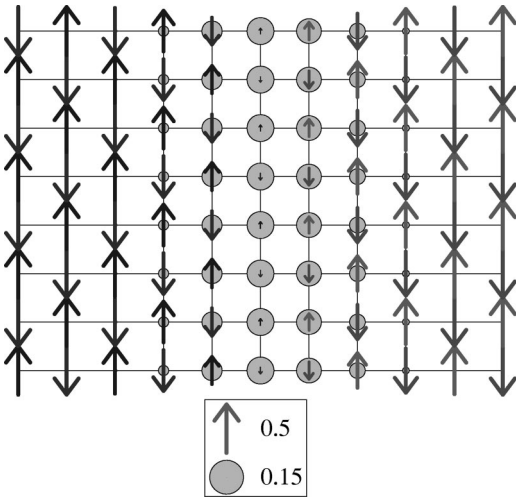


FIG. 17.  $11 \times 8$  cluster with four holes, cylindrical BC's, and  $J/t=0.35$ . The ground state contains a stripe.

Figures 14–17 show several examples of the states within the different clusters. Figure 14 shows the  $11 \times 6$  cluster with one hole, cylindrical BC's, and  $J/t=0.35$ . The ground state is homogeneous in this case. Figure 15 shows the same  $11 \times 6$  cluster with one hole, but with a staggered field applied at the open ends,  $J/t=0.35$ . The ground state is an ADW with the hole bound to it. Figure 16 shows the narrower  $11 \times 4$  cluster with one hole, no staggered field, cylindrical BC's, and at smaller  $J/t=0.2$ . The system spontaneously forms a stripe in the ground state for this system. One may conclude from here that in the  $11 \times L_y$  system with the number of holes  $N_h \approx L_y/4$  one will have a stripe in the ground state for  $J/t \leq 0.2$ . Figure 17 shows the largest  $11 \times 8$  cluster with four holes, no staggered field, cylindrical BC's, and  $J/t=0.35$ . In this case the ADW is also spontaneously formed with the holes occupying the border between the antiferromagnetic domains.

#### IV. RESULTS

##### A. Single-hole problem

The first problem we would like to clarify is the single-hole excitation problem in the stripe configuration. We therefore consider different clusters with an ADW induced by staggered fields for various values of  $J/t$ .

##### 1. Boundary conditions

We would like to remark here that simple cylindrical or periodic BC's do not quite work for the purpose of the study of the single excitation for the following reason. As we have discussed in Sec. II the core of the composite excitation is a holon, that is, an excitation carrying the kink, Fig. 5, while periodic BC's require the domain wall to be closed on itself around the cylinder, Fig. 18(a). This means that (i) there will be two excitations in the wall, holon and spinon, instead of one, Fig. 18(b), (ii) the free holon movement is frustrated by the spinon, (iii) periodic BC's induce an artificial (absent in  $L_y \rightarrow \infty$  limit) stripe meandering. The meandering is induced

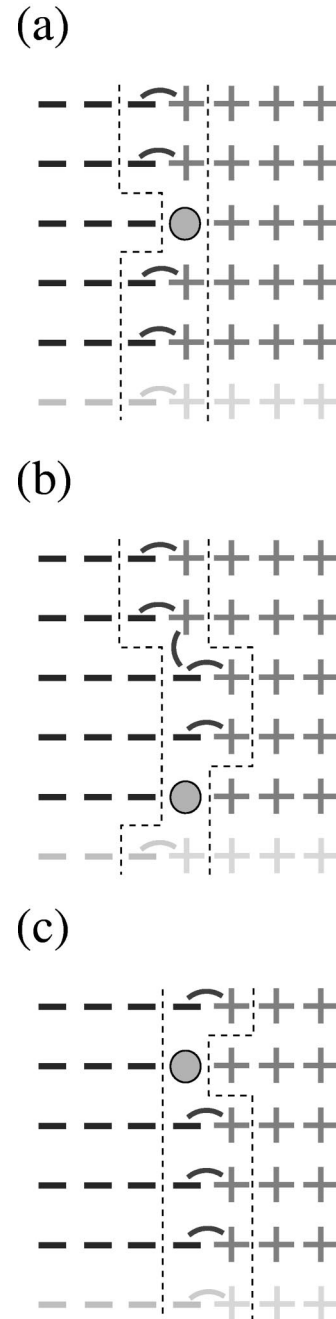


FIG. 18. A schematic picture of a  $7 \times 5$  cluster with periodic BC's and ADW. (a) One hole, straight ADW is enforced by periodic BC's, (b) holon and spinon in the straight ADW, (c) spinon and holon recombined after the circular motion of the hole around the cylinder, the ADW is translated in  $x$  direction as a result. The shaded row at the bottom is equivalent to the top row and is shown to emphasize periodic BC's in  $y$  direction.

by the process of holon recombination with the subsequent change of the side of the domain wall. Then, when the holon completes the full circle around the cylinder the whole domain wall is translated in the  $x$ -direction, Fig. 18(c).

The way to avoid such a frustration of the free holonic motion in the finite system is intuitively evident.<sup>73</sup> Since the

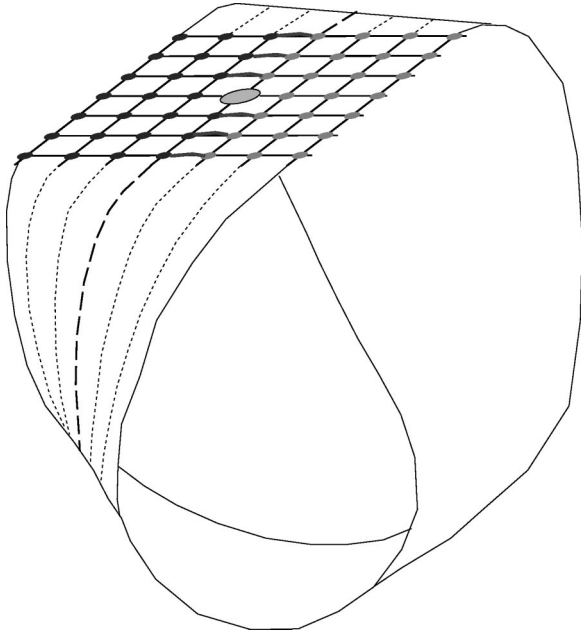


FIG. 19. A schematic view of  $7 \times 7$  cluster with Möbius BC's. An ADW in the center of the cluster and a wiggle are induced by Möbius BC's.

holon carries a topological (geometrical) charge the topological BC's are to be used. In our case it is Möbius BC's, Fig. 19. One can see that with these BC's the holon motion is unfrustrated. The number of sites should be odd to avoid the frustration in the spin system. For the case of the Möbius BC we, therefore, study clusters  $11 \times 7$ ,  $11 \times 5$ , and  $11 \times 3$ , and in the case of cylindrical BC's, the clusters are  $11 \times 8$ ,  $11 \times 6$ , and  $11 \times 4$ .

## 2. Energy

Figure 20 shows the  $J/t$  dependence of the ground-state energy of a single hole in the  $11 \times 7$  cluster with a Möbius BC, energy of the undoped system being subtracted. The theoretical curve shows the  $J/t$  dependence of the ground-state energy of the single holon spin polaron, that is, the energy of the bottom of the effective 1D band in Fig. 9,

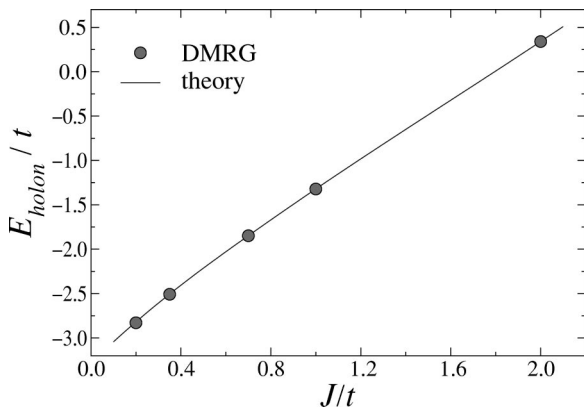


FIG. 20.  $J/t$  dependence of the ground-state energy of the single hole in  $11 \times 7$  cluster with Möbius BC (DMRG, circles) and the single holon spin polaron in the infinite stripe (theory, solid line).

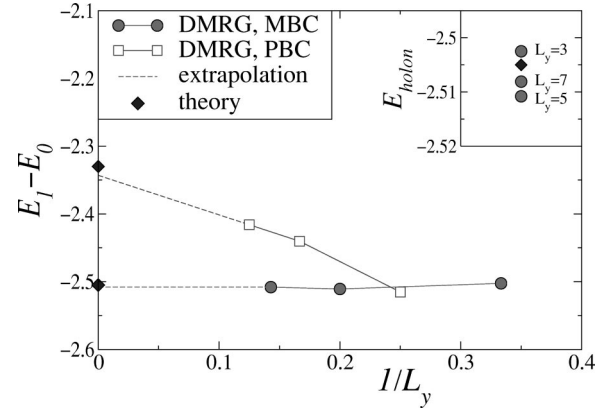


FIG. 21. The ground-state energy vs inverse linear size of the cluster. Möbius BC's (circles) correspond to the case of a single holon, periodic BC's (squares) induce the state with the holon and spinon. Theoretical results for the energy of the free holon and holon+spinon are put on the y axis (diamonds). Lines are guides to the eye. Inset shows Möbius BC's and theoretical data in a strongly magnified scale.  $J/t=0.35$ .

obtained from Eqs. (10)–(12). Note that the reference energy in Sec. II differs from that used here by the constant  $2J$ , the quantity associated with the energy of four bonds broken by the hole. We would like to note that there is no energy adjustment between numerical and analytical data used in Fig. 20 and it is not the result of the best fit. The maximal discrepancy of numerical and analytical results in Fig. 20 is about  $\sim 0.1\%$ . The closeness of agreement is even better than in the case of similar calculations for the spin polaron compared to the exact diagonalization data.<sup>20</sup> The reason for that has been discussed in Sec. II. The Trugman paths, which are beyond the retracable-path approximation, are the source of the discrepancies in the case of the spin polaron. In our case the Trugman paths do not exist in their original form.

One can also study the ground-state energy dependence on the size of the system. In Fig. 21 we show  $E_{GS}$  versus  $1/L_y$  for  $L_y=3,5,7$  (Möbius BC's) and for  $L_y=4,6,8$  (periodic BC's) together with the theoretical results for the infinite system,  $J/t=0.35$ . For the case of Möbius BC's the theoretical point at  $1/L_y=0$  is  $E_{GS}=E_{holon}$ ; for the case of periodic BC's the theoretical point represents the sum of the holon and spinon energy,  $E_{GS}=E_{holon}+J/2$ . That is, we assume that they do not form a bound state in the thermodynamic limit. One can see essentially negligible finite-size effects on the energy of the free holon spin polaron (Möbius BC's, also see inset). This feature can be anticipated since the excitation is a bandlike state and the ground-state wave vector belongs to the reciprocal space of all three clusters. The linear extrapolation to  $1/L_y=0$  in Fig. 21 was made from  $L_y=5,7$  and  $L_y=6,8$  for Möbius BC and periodic BC results, respectively.

## 3. Density

Figure 22 shows the results for the hole density distribution across the stripe for the ground state of the single hole at  $J/t=0.35$ . DMRG data from the  $11 \times 7$  cluster with Möbius BC's are shown by the circles. Theoretical results obtained

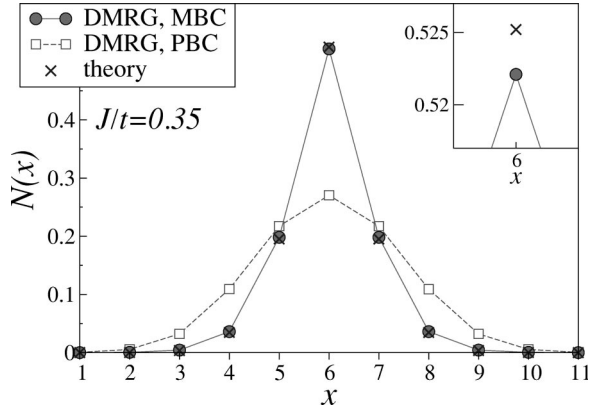


FIG. 22. Hole density distribution across the stripe at  $J/t=0.35$ . Data for Möbius BC's,  $11 \times 7$  cluster (circles), periodic BC's  $11 \times 8$  cluster, and theoretical results (crosses) are shown. Lines are guides to the eye. Inset shows Möbius BC's and theoretical data for  $x=6$  in a strongly magnified scale. Enlarged area is shown by the box.

from Eqs. (15)–(17) are shown by crosses. The total disagreement of the numerical Möbius BC data and analytical result is  $\sum_x |N_{num} - N_{th}| / N_{num} \approx 0.3\%$ . The same Fig. 22 shows the density profile of the hole distribution along the  $x$  axis for the case of periodic BC's. We note that the hole density modulation in the case of periodic BC's is essentially induced by the repulsion of the open boundaries in the  $x$  direction. If the system would be significantly wider in the  $x$  direction the circular meandering effect, which induces the transverse motion of the domain wall, would spread the density homogeneously. The same would be true in the case of periodic BC's in the  $x$  direction. This just demonstrates the following paradox: a finite system with periodic BC's in all directions would show a homogeneous ground state, as in Ref. 18, whose wave function may be, in fact, given by the superposition of slowly meandering stripes. In that case the stripe should be detected not from the density profile but from the instantaneous spin-spin correlation function, which should exhibit a strong antiphase component.

The density profile study of the single-hole problem is completed by the  $|\langle S^z \rangle(x)|$  data shown in Fig. 23. Note that the spin-density profile is not straightforwardly related to the hole density since there is also a large contribution from the hole-induced strings of misaligned spins affecting the average on-site spin values. For a single hole in the stripe of the length  $L_y$ , the suppression of the spin-density should be proportional to  $1/L_y$  ( $L_y=7$  in the case of the  $11 \times 7$  cluster). This is valid for all  $x$  except the center of the stripe, where the motion is holonic. Since the holon is a topological excitation it borders two 1D domains with opposite staggered spin value. Because of that any site along  $x=x_0$  ( $x_0=6$  in Fig. 23) always has average spin zero and this is not a  $1/L_y$  effect. The deviation of the theoretical results from DMRG for  $|\langle S^z \rangle(x)|$  is more observable than for  $N(x)$ . This is because of the subset of the paths which correspond to the processes of hole departing and then rejoining the stripe in the other leg of the ladder. Such paths can produce deviations from the  $1/L_y$  character of the spin-density modulation for

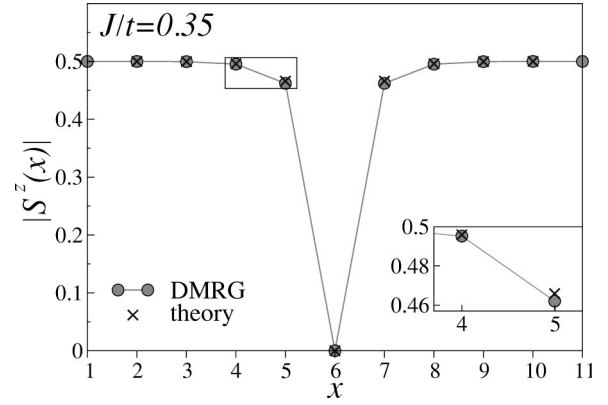


FIG. 23. The spin-density  $|\langle S^z \rangle(x)|$  vs  $x$  at  $J/t=0.35$ . Data for Möbius BC's,  $11 \times 7$  cluster (circles), and theoretical results (crosses) are shown. Lines are guides to the eye. Inset shows Möbius BC's and theoretical data for  $x=4$  and  $5$  in a magnified scale. Enlarged area is shown by the box.

$x \neq x_0$ , similar to that at  $x=x_0$ , which are hard to account for analytically. In any case, the largest discrepancy between the theory and numerical data for  $|\delta S^z(x=x_0 \pm 1)/S^z(x)|$  does not exceed 10%.

#### 4. Electron distribution function

The electron distribution function is compared as well. For this quantity the analytical calculations are quite cumbersome and were restricted by  $|\mathbf{d}|=2$  in Eq. (18). One can see from Eq. (18) that, apart from the constant,  $n_{\mathbf{k}}$  is given by the set of  $\cos(\mathbf{d} \cdot \mathbf{k})$ , with the coefficients given by the  $\sum_i \langle \tilde{c}_i^\dagger \tilde{c}_{i+\mathbf{d}} \rangle$  averages. We list such coefficients for several  $\mathbf{d}$ 's in Table I, where one can see a very good agreement of DMRG with the theory.

Figure 24 shows a plot of  $n_{\mathbf{k}}$  in the (1,0), (0,1), and (1,1) directions. A more informative 2D intensity plot in Fig. 25 shows the DMRG results for the electron distribution function averaged over the  $x$  and  $y$  directions,  $\bar{n}_{\mathbf{k}} = [n(k_x, k_y) + n(k_y, k_x)]/2$ . Two features are worth discussing.

First, there is almost no anisotropy between the  $k_x$  and  $k_y$  directions in  $n_{\mathbf{k}}$  for the highly anisotropic stripe configuration, Fig. 24. That can be, broadly speaking, interpreted as yet another demonstration of the equal importance of the transverse and longitudinal kinetic energies.<sup>74</sup> The broad features in  $n_{\mathbf{k}}$  in the  $t$ - $J$ -like models are understood as coming from the fast (incoherent) motion of the hole inside the quasiparticle, while the coherent part should show itself as a  $\delta$

TABLE I.  $\sum_i \langle \tilde{c}_i^\dagger \tilde{c}_{i+\mathbf{d}} \rangle$  for several coordination vectors  $\mathbf{d}$ .  $J/t=0.35$ .

$\mathbf{d}$	DMRG	Theory
(1,0)	0.1041	0.102
(0,1)	0.1216	0.115
(1,1)	-0.1266	-0.093
(2,0)	-0.0030	$\sim 0$
(0,2)	-0.0041	$\sim 0$

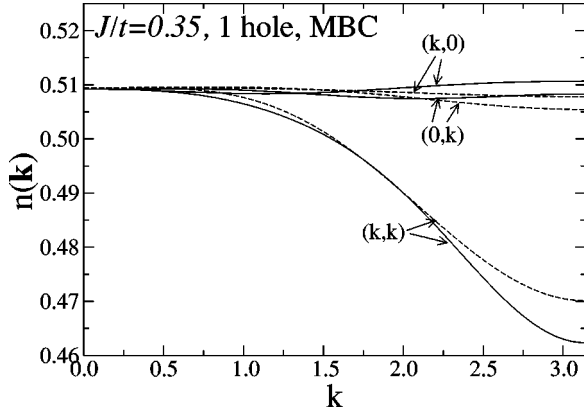


FIG. 24.  $n_{\mathbf{k}}$  for one-hole in Möbius BC  $11 \times 7$  cluster for  $(1,0)$ ,  $(0,1)$ , and  $(1,1)$  directions,  $J/t=0.35$ . Solid and dashed lines are DMRG and theory results, respectively.

peak at  $\mathbf{k}=\mathbf{k}_0$  proportional to the quasiparticle residue.<sup>35,68,69</sup> In the stripe case, excitations are not quasiparticles in a standard sense and, therefore, no sharp features are to be expected. In fact, it is easy to show that  $n_{\mathbf{k}}$  for a holon in a periodic 1D Ising chain is equal to

$$n_{\mathbf{k}} = \langle k_0 | \tilde{c}_{\mathbf{k}}^\dagger \tilde{c}_{\mathbf{k}} | k_0 \rangle = \frac{1}{2} - \frac{1}{L} \cos k \cos k_0, \quad (19)$$

where  $k_0$  is the momentum of the holon. This is the simple consequence of the fact that the holon is a zero-dimensional domain wall and that  $\langle \tilde{c}_i^\dagger \tilde{c}_{i+d} \rangle$  averages for distances larger than  $d=1$  are identically zero.

Second, the general behavior of  $n_{\mathbf{k}}$  in our problem is similar to that for the spin polaron: it has a maximum at  $\mathbf{k}=(0,0)$  and a minimum at  $\mathbf{k}=(\pi,\pi)$ , which is a simple consequence of the kinetic-energy minimization in the ground state.<sup>69</sup> However, its shape is crosslike rather than diamondlike (for the shape of spin-polaron  $n_{\mathbf{k}}$ , see Refs. 68 and 69). For spin polarons  $n_{\mathbf{k}}$  is mainly given by the powers of  $\gamma_{\mathbf{k}}=(\cos k_x$

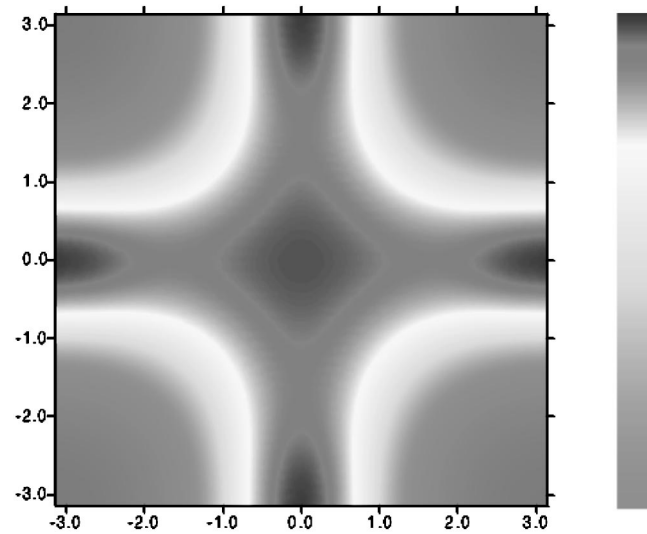


FIG. 25. 2D intensity plot of  $\bar{n}_{\mathbf{k}}=[n(k_x, k_y)+n(k_y, k_x)]/2$  from DMRG for a single hole in Möbius BC  $11 \times 7$  cluster,  $J/t=0.35$ .

$+\cos k_y)/2$ , which is zero along the lines  $(\pi,0)-(0,\pi)$ . This gives a diamondlike shape of  $n_{\mathbf{k}}$ . In the ADW configuration,  $\langle \tilde{c}_i^\dagger \tilde{c}_{i+d} \rangle$  for  $\mathbf{d}=(2,0)$  and  $(0,2)$  are strongly suppressed due to the  $\pi$  shift of the antiferromagnetic order parameter across the wall and across the holon. As a result, there are significant and almost equal  $\cos k_{x,y}$  and  $\cos k_x \cos k_y$  harmonics of opposite sign in  $n_{\mathbf{k}}$  (see Table I), but the harmonics  $\cos 2k_{x,y}$  are much suppressed. This is different from the spin-polaron case where they are all of the same order. Our results for  $n_{\mathbf{k}}$  in Fig. 25 are obtained for the single-hole problem in a stripe configuration, but since  $n_{\mathbf{k}}$  is saturated on short distances the same characteristic features should remain the same for higher doping. In fact, our “Maltese-cross-like” shape of  $n_{\mathbf{k}}$  is remarkably close to that observed in angle-resolved photoemission spectroscopy.<sup>75</sup>

Altogether, we have a very close agreement of the theory and DMRG data on the energy, density, and electron distribution function for the single excitation in the stripe configuration. This proves that our description of such an excitation is correct.

## B. Many-hole problem

The second problem we address in this work is the many-hole system. As we described in Sec. III the finite cluster can be doped with different amount of holes and one can use staggered-field BC’s at the open boundaries to enforce the state with and without an ADW. At some doping concentration the stripe state with an ADW becomes a ground state and no fields are necessary to stabilize it. We also note that for two and more holes the Möbius BC’s are not beneficial anymore because the holes play the role of boundaries for each other and the meandering of the domain wall can come as a result of some “collective” motion. Our Fig. 26 shows an example of such a process for the case of two holes. Such effects were discussed earlier in Refs. 55 and 63. However, we will show that the role of such processes in the stripe energy is negligible. This can be anticipated since the holes are spread significantly within the individual excitation and such collective processes should be statistically rare. Moreover, the bending of the stripe affects the free longitudinal motion of the holes and thus is unfavorable. This is in accord with the earlier work, Ref. 53, where such a rigidity was referred to as a *garden hose* effect. Note that in the case of a strictly 1D stripe close to complete filling ( $n_{\parallel} \approx 1$ ) the longitudinal kinetic energy is suppressed and the stripe meandering can become more important.<sup>55</sup>

### 1. Total energy

In Fig. 27 we show the DMRG and theory results for the total energy of the system per hole versus linear hole concentration  $n_{\parallel}=N_h/L_y$  (energy of the empty system being subtracted). DMRG data are obtained in the  $11 \times 8$  cluster with  $N_h=1,2,3,4,5$ , and 6 holes populating an ADW. At  $N_h > 3$  there was no need to stabilize the stripe by the fields at the boundaries since it was the ground state of the system. The theoretical curve is equivalent to the results shown in Fig. 10, which are obtained from the rigid-band filling of the effective 1D band using Eq. (13). Note again that the refer-

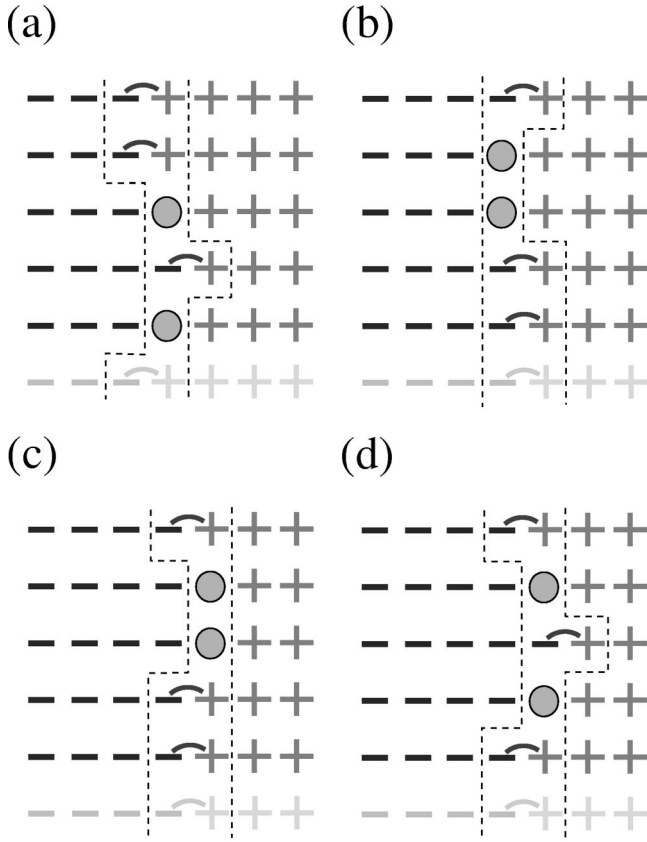


FIG. 26. A schematic picture of  $7 \times 5$  cluster with two holes in an ADW. (a)–(d) Hole motion in the periodic direction combined with the transverse motion of both holes results in the translation of ADW in  $x$  direction. The shaded row at the bottom is equivalent to the top row and is shown to emphasize periodic BC's in  $y$  direction.

ence energy is different from Sec. II by  $2J$ . Crosses are also the result for the same rigid-band filling but for the system with the discrete  $\mathbf{k}$  space. We mimic the periodic finite-size system by imposing that only  $L_y = 8$   $\mathbf{k}$  points are available in the effective 1D band. Straight solid and dashed lines are the energies per hole of the systems of independent spin polarons and bound states of spin polarons in the homogeneous AF, respectively.

Obviously, the rigid-band filling neglects the effects of interaction between the carriers except the Fermi repulsion. Such interactions are quite complicated and would include attractive as well as repulsive terms as well as some collective effects resulting in stripe meandering. However, given the good agreement of analytical and numerical results one can conclude that such effects are secondary for the stripe formation. Therefore, the kinetic energy of the individual holes, both along the stripe (holonic motion) and perpendicular to it (spin-polaron part), is the main reason that brings the stripe to the ground state. Note that since the holons are spinless, the Fermi exclusion is much more effective at inducing proper correlations between holons, acting as a hardcore repulsion, than in the usual spin-1/2 case, where up- and down-spin particles can be on the same site. Thus, the effectiveness of this simple band-filling approach is not so surprising.

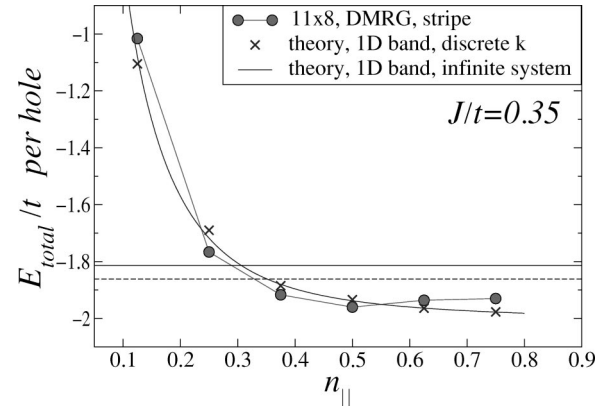


FIG. 27. Total energy of the system with an ADW per hole versus  $n_{\parallel}$ . Circles are the DMRG results from the  $11 \times 8$  cluster. Solid curve and crosses are the theoretical results as described in the text. Horizontal solid and dashed lines are the energies of free spin polarons and bound states of spin polarons in the homogeneous AF, respectively.  $J/t = 0.35$ .

One can question the physical picture of a straight, weakly meandering stripe described by an effective 1D band from the point of view of applicability of the free-holon approximation.<sup>63</sup> The controversy is that at the physically relevant concentration  $n_{\parallel} \approx 0.5$  the free-holon approximation ( $n_{\parallel} \ll 1$ ) and the free-electron approximation ( $1 - n_{\parallel} \ll 1$ ) are not applicable and should be equally bad. A very good agreement of our theory with the numerical data up to  $n_{\parallel} \sim 0.5$  and beyond can be seen as quite puzzling since the theory is based on  $n_{\parallel} \ll 1$  approach. However, such a controversy comes from the mean-field picture of the strictly 1D stripe. One should rather consider a stripe to be a combination of strongly dressed, well spread holes forming a collective bound state with the ADW. In fact, the actual amount of holons within the effective 1D band is given by  $n_{holons} = \sum_{k_y < k_F} Z_{k_y}$  ( $Z_{k_y}$  is a residue of the Green's function), which, for the physical range of parameters, does not exceed  $n_{holons} \approx 0.2 \ll 1$  even for a completely filled stripe  $n_{\parallel} = 1$ . It demonstrates that the  $n_{\parallel} \ll 1$  approach should work well in all ranges of doping.

## 2. Chemical potential

Figure 27 provided a comparison of the total energy of the system within the different topological sectors, which defines the ground state. However, a more discrete energetic analysis is necessary to study the delicate balance of the stripe formation. Here we introduce the chemical potential as the difference between the energy of the system with  $N_h$  and  $N_h - 1$  number of holes:

$$\mu(N_h) = E_{tot}^{N_h} - E_{tot}^{N_h - 1}. \quad (20)$$

In the situation when the kinetic energy is frustrated, it gives a measure of how effectively the energy of the system is lowered by an extra hole for the states with different topology.

Figure 28 shows  $\mu$  as a function of  $N_h$  for the DMRG in the  $11 \times 8$  cluster with cylindrical BC's for the states with and

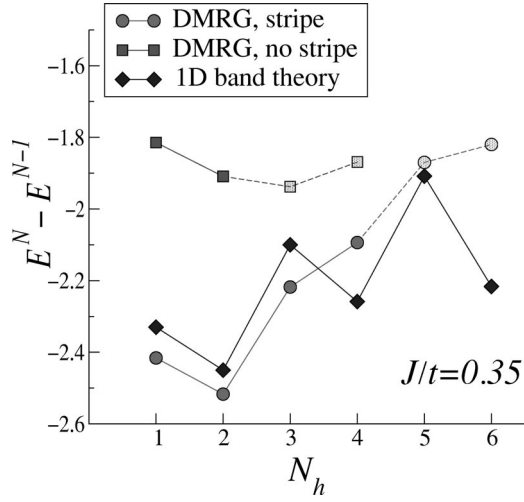


FIG. 28. Chemical potential vs  $N_h$ . Discrete- $k$  rigid-band results,  $L_y=8$ , (diamonds), DMRG data in  $11 \times 8$  cluster for the system with ADW (circles) and without ADW (squares),  $J/t=0.35$ . Lines are guides to the eye.

without the stripe, together with theoretical results calculated from the discrete- $k$  rigid-band filling of the effective 1D stripe band. In obtaining theoretical data points we needed to account for the frustrating character of the cylindrical BC's (discussed above for one hole) for the cases when the number of holes is odd:

$$E_{tot}^{N_h} = \sum_{n=1}^{N_h} E_{kin}(k_n) + (3J/2)N_h + (J/2)\delta_{N_h, \text{odd}}, \quad (21)$$

where  $k_n$  is one of the available  $L_y=8$   $\mathbf{k}$  points, counted from the bottom of the band,  $E_{kin}(k_n)$  is the energy of the 1D excitation, Fig. 9,  $3J/2$  is the energy of the static hole at the ADW,  $J/2 = E_{spinon}$  is the frustration energy caused by BC's. As a result, the theoretical expression for the chemical potential is given by

$$\mu^{th}(N_h) = E_{kin}(k_{N_h}) + 3J/2 + (J/2)(-1)^{N_h}, \quad (22)$$

where  $E_{kin}(k_{N_h})$  is the lowest energy available for the  $N_h$  hole in the 1D band. The last term provides a zigzag behavior of  $\mu(N_h)$  shown in Fig. 28.

For  $N_h=1$  the DMRG and the theory points are equivalent to those in Fig. 21 for the  $L_y=8$  cluster with periodic BC's and for the  $E_{th}^{GS} = E_{holon} + E_{spinon}$ , respectively. Since the DMRG data in Fig. 21 seem to scale to  $E_{th}^{GS}$ , the difference  $\mu^{DMRG}(1) - \mu^{theory}(1)$  is, most probably, a finite-size effect. One can see a very good overall agreement of the trends in both the numerical and analytical result. Since the theoretical results are calculated from the picture which corresponds to the subsequent filling of the 1D band, the chemical potential should grow as the higher  $k$  states are filled.

We mark differently the data for  $N_h=5$  and  $N_h=6$  since in the  $L_y=8$  stripe they correspond to the high concentrations where the finite-size effects become more pronounced. Note again that the ADW configuration (stripe) is enforced

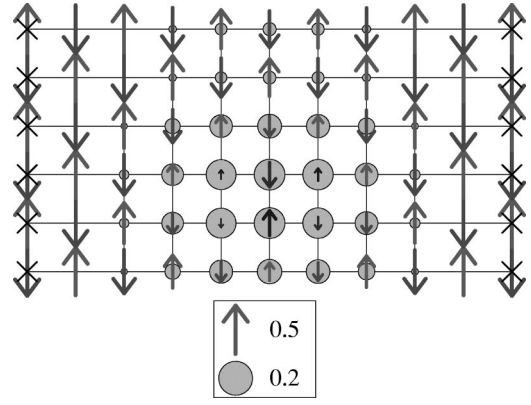


FIG. 29.  $11 \times 6$  cluster with four holes. Homogeneous antiferromagnetic state is enforced by the boundary conditions. Instead of being homogeneous, the circular ADW is created.

by the boundary conditions at  $N_h=1,2$ , while for  $N_h=4,5,6$  it is the ground state. Conversely, the no-stripe state (homogeneous AF) is the ground state for  $N_h=1,2$  ( $N_h=3$  looks like a metastable state) and is to be enforced for  $N_h > 2$ . We mark the no-stripe data for  $N_h=3,4$  as shaded because the  $N_h=4$  state is not formed by the gas of spin polarons or polaron pairs but rather is a stripelike circle with an ADW in the center of the cluster (Fig. 29). It is not a bound state of polaron pairs, but rather a many-particle bound state with the condensate of magnons, the ‘‘droplet’’ of the  $\pi$ -shifted AF inside the circle corresponds to such a condensate. This shows the strong tendency to the stripe formation such that even a small, finite number of holes will prefer to form a closed loop of the ADW nuclei, which can then develop into the straight stripes as the doping grows. We would like to discuss here the  $N_h=1$  and  $N_h=2$  cases in Fig. 28 in more detail. While the no-stripe state is the ground state for these hole concentrations, the effectiveness of the energy lowering is much higher in the stripe state. For  $N_h=1$  it is yet another form of the discussion given in Sec. II that at the bottom of the 1D holon-spin-polaron band the energy is significantly lower than in the bulk. In other words, from Fig. 28 one can see that the individual charge carriers benefit energetically from being at the stripe. Since for  $N_h=1$  in either the stripe or the no-stripe system it is the kinetic energy of the individual charge excitation which is optimized, one can conclude that the formation of the stripe is kinetic-energy driven.

The idea that stripe formation can be viewed as a condensation of a set of hole pairs has been discussed in Ref. 76. Here we see that if one preconfigures the ADW, even a single hole is bound to it with substantial binding energy, and pairing is not involved. The quantitative description of stripe formation that we have developed, which does not involve pairing, suggests that pairing is a lower-energy phenomena which can be considered after the stripe is formed. However, the condensation of pairs idea may also be a valid point of view. An energetic test for this point of view would be that the energy per hole of a stripe should be only slightly less than that of separate pairs. More specifically, the energy advantage of the stripe should be less than the pair binding



energy. For the  $11 \times 8$ ,  $J/t=0.35$  system, we find that the energy of the half-filled stripe, per pair of holes, is  $2E_{1/2}^{stripe}/N_h = -3.91$ . This compares with  $E_2 = -3.72$  for a single pair. The difference between these two energies is approximately twice the binding energy of a pair of holes,  $\Delta \approx -0.09$ , suggesting that the condensation of hole pairs is not nearly as good a description as the current formalism, at least in the  $t$ - $J_z$  model.

A separate issue is whether the stripes help to promote pairing, are irrelevant to it, or hinder it. In the no-stripe state the chemical potential is lower for  $N_h=2$  than for  $N_h=1$ . This energy is the true bound-state energy of the pair of spin polarons  $\Delta_{sp} = \mu(2) - \mu(1) < 0$ , much studied in the past.<sup>20</sup> In the stripe state the excitations do not form a true bound state, although  $\mu(2) - \mu(1) < 0$ . The theoretical result for this difference,  $\mu(2) - \mu(1) = E_{kin}(k_2) - E_{kin}(k_1) - J$ , contains the negative energy  $-J$  provided by the removal of the spinon, which is induced by the PBC's in the one-hole system and has nothing to do with the pairing. Since the DMRG data look very much the same and also  $\mu^{DMRG}(2) - \mu^{theory}(2)$  is almost the same as for the one-hole case, one may conclude that there is no binding involved here at all. However, it may also be that the binding energy is compensating the stronger finite-size effects for the  $N_h=2$  case leading to the same  $\mu^{DMRG}(2) - \mu^{theory}(2)$ . In any case, we see no significant enhancement of binding and thus the stripes seem to be largely irrelevant to pair binding.

The collective stripe fluctuations (as opposed to the fluctuations of individual holes) have been discussed as an effective alternative way to lower the energy and stabilize the stripe phase.<sup>55</sup> We check the effectiveness of such processes by studying two holes in the  $11 \times 8$  system with periodic BC's and Möbius BC's. The Möbius BC's suppress the stripe meandering considerably, which is seen in the hole density profiles, while the difference between the energies of the states is slightly above the numerical accuracy of the DMRG.

The overall conclusion of this discussion is the following. The kinetic energy of the *individual* charge excitations at the domain wall, which includes significant components of both longitudinal and transverse motion, is the reason for the stripe formation. The pairing energy does not seem to be significantly modified and, in general, is associated with the smaller energy scale. Meandering of the stripe, while being important for some other properties, has very little effect on the energy of the stripe. Therefore, one can write this as a hierarchy of the energy scales:

$$\Delta E_{kin} \gg E_{pairing} \gg E_{meandering}, \quad (23)$$

where  $\Delta E_{kin}$  is the *difference* in the release of the kinetic energies between the stripe and homogeneous state,  $\Delta E_{kin} \sim (J^2 t)^{1/3}$ , as discussed in Sec. II.  $E_{pairing} \sim J$  but, in fact, is only a fraction of  $J$ .<sup>20</sup>  $E_{meandering}$  should carry a statistically small factor describing the probability of the collective motion of two or more holes together. As we mentioned,  $E_{meandering}$  is hardly detectable numerically.

The emerging picture of the stripe as a collective bound state of strongly dressed 1D band excitations with the ADW

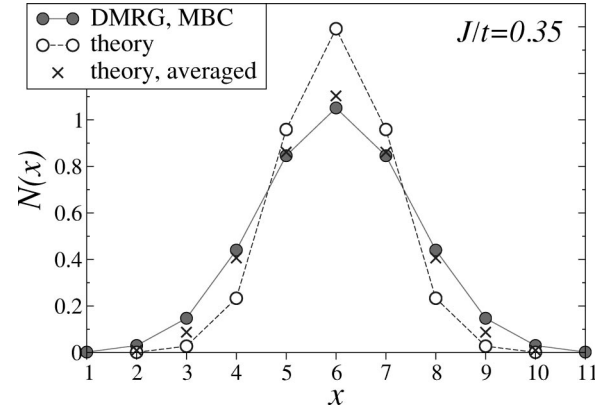


FIG. 30. Hole density distribution across the stripe at  $J/t = 0.35$ . DMRG data for four holes in  $11 \times 8$  cluster, cylindrical BC's (filled circles). Theoretical results for (i) a half-filled stripe centered at  $x_0=6$  (empty circles), (ii) linear combination of stripes at  $x_0 = 5$ ,  $x_0=6$ , and  $x_0=7$  (crosses) are shown. Lines are guides to the eye.

also implies that there are deep states, which reduce the energy of the stripe, and shallow states, which are spread around the stripe and are only weakly coupled to it.

### 3. Density

To conclude this section we show the hole density profile for the half-filled stripe in the  $11 \times 8$  cluster (four holes) compared to the theoretical results for  $n_{\parallel}=1/2$  from Eqs. (14)–(16),  $J/t=0.35$ , Fig. 30. In DMRG data cylindrical BC's are used and the stripe is the ground state for this system. Theoretical results for the 1D-band stripe centered in the middle of the system at  $x_0=6$  are shown by the empty circles. As we discussed before, the meandering effect causes the migration of the stripe as a whole in the transverse direction. Since we know that the meandering effect is weak and that it effectively leads to the coupling of stripes centered at the different  $x_0$  we, therefore, model this effect by assuming that the ground state is given by the linear superposition of 1D bands centered at  $x=5$ ,  $6$ , and  $7$  with equal weight. Further distribution is assumed to be unfavorable because of the open BC's. Then the density profile is given by the average:  $\bar{N}(x) = [N_{x_0=5}(x) + N_{x_0=6}(x) + N_{x_0=7}(x)]/3$ . The results of such an averaging are also shown in Fig. 30 (crosses). Even better agreement can be reached assuming wider meandering and weight distribution, but such a task is beyond the scope of this work.

## V. CONCLUSIONS

Summarizing, we have presented a comprehensive comparison of the DMRG numerical data for clusters up to  $11 \times 8$  with the analytical studies based on the self-consistent Green's-function method for a single stripe of holes in an AF described by the  $t$ - $J_z$  model. We consider the close agreement of the results as a strong support for the validity of our analytical method and of the physical picture which follows from it. We have provided a description of the charge carriers building the stripe as a system of 1D elementary

excitations, unifying the features of holons and antiferromagnetic spin polarons. Then the stripe should be seen as an effective 1D band partly filled with these elementary excitations. This picture is in a very good accord with the numerical data.

As it follows from our study, the stripe can be roughly described by the deep backbone states, which minimize the energy of the antiphase configuration in the AF and the shallow, almost free spin-polaron-like excitations around the ADW. Since the spin polarons are known to have a considerable pairing between themselves, such a framework does not require the superconducting pairing to come from some 1D instability, but rather suggests that the pairing is largely unrelated to the 1D stripe pattern. Such a scenario is also discussed in recent work, Ref. 77. Another hypothetical advantage of our picture is a more effective screening of the long-range component of the Coulomb repulsion, which represents the problem for the system of strictly 1D charges.<sup>78</sup>

Altogether, the comprehensive comparison of the results of the theory and DMRG numerical approach has shown a very close quantitative agreement, thus providing a strong support to our way of understanding the charge excitations at the antiphase stripe in an AF.

#### ACKNOWLEDGMENTS

We would like to acknowledge invaluable discussions with A. Abanov, E. Dagotto, L. Pryadko, O. Tchernyshyov, J. Tranquada, and S. Trugman. We are indebted to A. Bishop for numerous stimulating conversations. This research was supported in part by Oak Ridge National Laboratory, managed by UT-Battelle, LLC, for the U.S. Department of Energy under Contract No. DE-AC05-00OR22725, and by a CULAR research grant under the auspices of the U.S. Department of Energy. S.R.W. acknowledges the support of the NSF through Grant No. DMR 98-70930.

\*Also at Institute of Semiconductor Physics, Novosibirsk, Russia.

<sup>1</sup>For reviews see, e.g., D. Pines, *Physica C* **282**, 273 (1997); P. W. Anderson, *Adv. Phys.* **46**, 3 (1997).

<sup>2</sup>D. J. Scalapino, E. Loh, and J. E. Hirsch, *Phys. Rev. B* **34**, 8190 (1986); D. J. Scalapino, *Phys. Rep.* **250**, 329 (1995); N. Bulut and D. J. Scalapino, *Phys. Rev. B* **54**, 14971 (1996).

<sup>3</sup>E. Dagotto and J. Riera, *Phys. Rev. Lett.* **70**, 682 (1993); D. Poilblanc, J. Riera, and E. Dagotto, *Phys. Rev. B* **49**, 12318 (1994); Y. Ohta, T. Shimozato, R. Eder, and S. Maekawa, *Phys. Rev. Lett.* **73**, 324 (1994).

<sup>4</sup>M. Yu. Kagan and T. M. Rice, *J. Phys.: Condens. Matter* **6**, 3771 (1994).

<sup>5</sup>V. V. Flambaum, M. Yu. Kuchiev, and O. P. Sushkov, *Physica C* **227**, 267 (1994); V. I. Belinicher, A. L. Chernyshev, A. V. Dotsenko, and O. P. Sushkov, *Phys. Rev. B* **51**, 6076 (1995); N. M. Plakida, P. Horsch, A. Liechtenstein, and V. S. Oudovenko, *Phys. Rev. B* **55**, 11997 (1997).

<sup>6</sup>A. Nazarenko, K. J. E. Vos, S. Haas, E. Dagotto, and R. J. Gooding, *Phys. Rev. B* **51**, 8676 (1995).

<sup>7</sup>V. I. Belinicher, A. L. Chernyshev, and V. A. Shubin, *Phys. Rev. B* **53**, 335 (1996); P. W. Leung, B. O. Wells, and R. J. Gooding, *ibid.* **56**, 6320 (1997).

<sup>8</sup>C. Kim, P. J. White, Z.-X. Shen, T. Tohyama, Y. Shibata, S. Maekawa, B. O. Wells, Y. J. Kim, R. J. Birgeneau, and M. A. Kastner, *Phys. Rev. Lett.* **80**, 4245 (1998), and references therein.

<sup>9</sup>J. M. Tranquada, B. J. Sternlieb, J. D. Axe, Y. Nakamura, and S. Uchida, *Nature (London)* **375**, 561 (1995); J. M. Tranquada, J. D. Axe, N. Ichikawa, Y. Nakamura, S. Uchida, and B. Nachumi, *Phys. Rev. B* **54**, 7489 (1996).

<sup>10</sup>S.-W. Cheong, G. Aeppli, T. E. Mason, H. Mook, S. M. Hayden, P. C. Canfield, Z. Fisk, K. N. Clausen, and J. L. Martinez, *Phys. Rev. Lett.* **67**, 1791 (1991); A. Bianconi, N. L. Saini, T. Rossetti, A. Lanzara, A. Perali, M. Missori, H. Oyanagi, H. Yamaguchi, Y. Nishihara, and D. H. Ha, *Phys. Rev. B* **54**, 12018 (1996); A. Lanzara *et al.*, *J. Supercond.* **10**, 319 (1997); S. Wakimoto, G. Shirane, Y. Endoh, K. Hirota, S. Ueki, K. Yamada, R. J. Birgeneau, M. A. Kastner, Y. S. Lee, P. M. Gehring, and S. H. Lee, *Phys. Rev. B* **60**, R769 (1999).

<sup>11</sup>E. Dagotto, *Rev. Mod. Phys.* **66**, 763 (1994), and references therein.

<sup>12</sup>A. S. Mishchenko, N. V. Prokof'ev, and B. V. Svistunov, *Phys. Rev. B* **64**, 033101 (2001).

<sup>13</sup>S. R. White and I. Affleck, *Phys. Rev. B* **64**, 024411 (2001).

<sup>14</sup>P. W. Leung, *Phys. Rev. B* **65**, 205101 (2002).

<sup>15</sup>P. W. Leung, *Phys. Rev. B* **62**, 6112 (2000); D. A. Ivanov, P. A. Lee, and X.-G. Wen, *Phys. Rev. Lett.* **84**, 3958 (2000).

<sup>16</sup>J. Zaanen and O. Gunnarsson, *Phys. Rev. B* **40**, 7391 (1989); H. J. Schulz, *J. Phys. (France)* **50**, 2833 (1989); D. Poilblanc and T. M. Rice, *Phys. Rev. B* **39**, 9749 (1989); K. Machida, *Physica C* **158**, 192 (1989); M. Kato, K. Machida, H. Nakanishi, and M. Fujita, *J. Phys. Soc. Jpn.* **59**, 1047 (1990).

<sup>17</sup>S. R. White and D. J. Scalapino, *Phys. Rev. Lett.* **80**, 1272 (1998); **81**, 3227 (1998); **84**, 3021 (2000).

<sup>18</sup>C. S. Hellberg and E. Manousakis, *Phys. Rev. Lett.* **83**, 132 (1999).

<sup>19</sup>Some preliminary results were reported in conference proceedings, *Physica B* **312-313**, 566 (2002).

<sup>20</sup>A. L. Chernyshev and P. W. Leung, *Phys. Rev. B* **60**, 1592 (1999).

<sup>21</sup>A. L. Chernyshev, A. H. Castro Neto, and A. R. Bishop, *Phys. Rev. Lett.* **84**, 4922 (2000).

<sup>22</sup>P. W. Anderson, *Science* **235**, 1196 (1987); C. Gros, R. Joynt, and T. M. Rice, *Phys. Rev. B* **36**, 381 (1987); F. C. Zhang and T. M. Rice, *Phys. Rev. B* **37**, 3759 (1988).

<sup>23</sup>C. L. Kane, P. A. Lee, and N. Read, *Phys. Rev. B* **39**, 6880 (1988); S. Schmitt-Rink, C. M. Varma, and A. E. Ruckenstein, *Phys. Rev. Lett.* **60**, 2793 (1988); F. Marsiglio, A. E. Ruckenstein, S. Schmitt-Rink, and C. M. Varma, *Phys. Rev. B* **43**, 10882 (1991); G. Martínez and P. Horsch, *Phys. Rev. B* **44**, 317 (1991); Z. Liu and E. Manousakis, *ibid.* **45**, 2425 (1992); **51**, 3156 (1995); A. Ramsak and P. Horsch, *ibid.* **48**, 10559 (1993); **57**, 4308 (1998); N. M. Plakida, V. S. Oudovenko, and V. Yu. Yushankhai, *ibid.* **50**, 6431 (1994); J. Bala, A. M. Oleś, and J. Zaanen, *ibid.* **52**, 4597 (1995); H. Barentzen and V. Oudovenko, *Europhys. Lett.* **47**, 227 (1999).

<sup>24</sup>B. Shraiman and E. Siggia, *Phys. Rev. Lett.* **60**, 740 (1988).

<sup>25</sup>R. Eder and K.W. Becker, *Z. Phys. B: Condens. Matter* **78**, 219 (1990).

- <sup>26</sup>Y. Lu, Chin. J. Phys. (Taipei) **31**, 579 (1993).
- <sup>27</sup>G. Reiter, Phys. Rev. B **49**, 1536 (1994).
- <sup>28</sup>O. A. Starykh and G. F. Reiter, Phys. Rev. B **53**, 2517 (1996).
- <sup>29</sup>T. Barnes, E. Dagotto, A. Moreo, and E. S. Swanson, Phys. Rev. B **40**, 10977 (1989); J. A. Riera and E. Dagotto, *ibid.* **47**, 15346 (1993); D. Poilblanc, H. J. Schulz, and T. Ziman, *ibid.* **46**, 6435 (1992).
- <sup>30</sup>V. I. Belinicher, A. L. Chernyshev, and V. A. Shubin, Phys. Rev. B **56**, 3381 (1997); A. L. Chernyshev, A. Dotsenko, and O. Sushkov, *ibid.* **49**, 6197 (1994).
- <sup>31</sup>S. R. White and D. J. Scalapino, Phys. Rev. B **55**, 6504 (1997).
- <sup>32</sup>C. J. Hamer, Z. Weihong, and J. Oitmaa, Phys. Rev. B **58**, 15508 (1998).
- <sup>33</sup>J. R. Schrieffer, X. G. Wen, and S. C. Zhang, Phys. Rev. B **39**, 11663 (1989); D. M. Frenkel and W. Hanke, *ibid.* **42**, 6711 (1990).
- <sup>34</sup>B. I. Shraiman and E. D. Siggia, Phys. Rev. B **40**, 9162 (1989); **42**, 2485 (1990).
- <sup>35</sup>A. L. Chernyshev, P. W. Leung, and R. J. Gooding, Phys. Rev. B **58**, 13594 (1998), and references therein.
- <sup>36</sup>L. N. Bulaevskii, E. L. Nagaev, and D. I. Khomskii, Sov. Phys. JETP **27**, 638 (1967); W. F. Brinkman and T. M. Rice, Phys. Rev. B **2**, 1324 (1970).
- <sup>37</sup>R. Eder, Phys. Rev. B **45**, 319 (1992); P. Wróbel and R. Eder, *ibid.* **49**, 1233 (1994); **58**, 15160 (1998).
- <sup>38</sup>M. Yu. Kuchiev and O. P. Sushkov, Physica C **218**, 197 (1993).
- <sup>39</sup>D. J. Scalapino, J. Low Temp. Phys. **117**, 179 (1999).
- <sup>40</sup>O. P. Sushkov, Phys. Rev. B **49**, 1250 (1994).
- <sup>41</sup>O. P. Sushkov, Phys. Rev. B **63**, 174429 (2001).
- <sup>42</sup>D. Poilblanc, Phys. Rev. B **52**, 9201 (1995).
- <sup>43</sup>J. Igarashi and P. Fulde, Phys. Rev. B **45**, 12357 (1992); G. Khasliullin and P. Horsch, *ibid.* **47**, 463 (1993); F. P. Onufrieva, V. P. Kushnir, and B. P. Toperverg, *ibid.* **50**, 12935 (1994).
- <sup>44</sup>B. Shraiman and E. Siggia, Phys. Rev. Lett. **62**, 1564 (1989).
- <sup>45</sup>T. Dombre, J. Phys. (France) **51**, 847 (1990).
- <sup>46</sup>O. P. Sushkov, Phys. Rev. B **54**, 9988 (1996).
- <sup>47</sup>P. Prelovsek and X. Zotos, Phys. Rev. B **47**, 5984 (1993); P. Prelovsek and I. Sega, *ibid.* **49**, 15241 (1994).
- <sup>48</sup>S. A. Kivelson and V. J. Emery, Synth. Met. **80**, 151 (1996).
- <sup>49</sup>V. J. Emery, S. A. Kivelson, and O. Zachar, Phys. Rev. B **56**, 6120 (1997).
- <sup>50</sup>A. H. Castro Neto, Z. Phys. B: Condens. Matter **103**, 185 (1997).
- <sup>51</sup>A. H. Castro Neto and D. Hone, Phys. Rev. Lett. **76**, 2165 (1996).
- <sup>52</sup>M. I. Salkola, V. J. Emery, and S. A. Kivelson, Phys. Rev. Lett. **77**, 155 (1996); J. Zaanen, O. Y. Osman, and W. van Saarloos, Phys. Rev. B **58**, R11868 (1998); M. Vojta and S. Sachdev, Phys. Rev. Lett. **83**, 3916 (1999).
- <sup>53</sup>C. Nayak and F. Wilczek, Phys. Rev. Lett. **78**, 2465 (1997).
- <sup>54</sup>R. B. Laughlin, cond-mat/9802180 (unpublished); Phys. Rev. Lett. **79**, 1726 (1997); P. W. Anderson, Phys. Rev. B **55**, 11785 (1997).
- <sup>55</sup>J. Zaanen, J. Phys. Chem. Solids **59**, 1769 (1998); J. Zaanen, O. Y. Osman, H. V. Kruis, Z. Nussinov, and J. Tworzydło, Philos. Mag. B **81**, 1485 (2001).
- <sup>56</sup>G. B. Martins, R. Eder, and E. Dagotto, Phys. Rev. B **60**, R3716 (1999); G. B. Martins, C. Gazza, J. C. Xavier, A. Feiguin, and E. Dagotto, Phys. Rev. Lett. **84**, 5844 (2000); G. B. Martins, C. Gazza, and E. Dagotto, Phys. Rev. B **62**, 13926 (2000); G. B. Martins, J. C. Xavier, C. Gazza, M. Vojta, and E. Dagotto, *ibid.* **63**, 014414 (2001).
- <sup>57</sup>P. Wróbel and R. Eder, Phys. Rev. B **62**, 4048 (2000); P. Wróbel and R. Eder, Int. J. Mod. Phys. B **14**, 3765 (2000); **14**, 3759 (2000).
- <sup>58</sup>A. G. Abanov and P. B. Wiegmann, hep-th/0105213 (unpublished).
- <sup>59</sup>W. P. Su, J. R. Schrieffer, and A. J. Heeger, Phys. Rev. B **22**, 2099 (1980); A. J. Heeger, S. Kivelson, J. R. Schrieffer, and W. P. Su, Rev. Mod. Phys. **60**, 781 (1988).
- <sup>60</sup>M. A. Kastner, R. J. Birgeneau, G. Shirane, and Y. Endoh, Rev. Mod. Phys. **70**, 897 (1998).
- <sup>61</sup>L. P. Pryadko, S. A. Kivelson, V. J. Emery, Y. B. Bazaliy, and E. A. Demler, Phys. Rev. B **60**, 7541 (1999).
- <sup>62</sup>H. J. Schulz, Int. J. Mod. Phys. B **5**, 57 (1991); H. Shiba and M. Ogata, Prog. Theor. Phys. **108**, 265 (1992).
- <sup>63</sup>O. Tchernyshyov and L. P. Pryadko, Phys. Rev. B **61**, 12503 (2000); cond-mat/9907472 (unpublished).
- <sup>64</sup>E. W. Carlson, S. A. Kivelson, Z. Nussinov, and V. J. Emery, Phys. Rev. B **57**, 14704 (1998).
- <sup>65</sup>S. Trugman, Phys. Rev. B **37**, 1597 (1988).
- <sup>66</sup>A. V. Balatsky and Z. X. Shen, Science **284**, 1137 (1999).
- <sup>67</sup>The problem of the stripe stability to the untwist of the order parameter has been studied as well, Ref. 21.
- <sup>68</sup>A. Ramsak, I. Sega, and P. Prelovsek, Phys. Rev. B **61**, 4389 (2000); J. Riera and E. Dagotto, *ibid.* **55**, 14543 (1997).
- <sup>69</sup>R. Eder and K.W. Becker, Phys. Rev. B **44**, 6982 (1991); R. Eder and P. Wróbel, *ibid.* **47**, 6010 (1993).
- <sup>70</sup>We thank Elbio Dagotto for questioning this issue.
- <sup>71</sup>A. A. Ovchinnikov, Zh. Éksp. Teor. Fiz. **64**, 342 (1973) [Sov. Phys. JETP **37**, 176 (1973)].
- <sup>72</sup>We are grateful to Sasha Abanov for this example.
- <sup>73</sup>The same BC's were used to avoid the frustration of the hole motion in the spin-ladder system, T. F. A. Müller and T. M. Rice, Phys. Rev. B **58**, 3425 (1998).
- <sup>74</sup>The same conclusion has been reached recently based on energetic analysis of the stripe in the  $t$ - $J$  model studied by DMRG, A. P. Kampf, D. J. Scalapino, and S. R. White, Phys. Rev. B **64**, 052509 (2001).
- <sup>75</sup>X. J. Zhou, P. Bogdanov, S. A. Kellar, T. Noda, H. Eisaki, S. Uchida, Z. Hussain, and Z.-X. Shen, Science **286**, 268 (1999).
- <sup>76</sup>S. R. White and D. J. Scalapino, cond-mat/9610104 (unpublished).
- <sup>77</sup>A. H. Castro Neto, Phys. Rev. B **64**, 104509 (2001).
- <sup>78</sup>A. S. Alexandrov and V. V. Kabanov, Pis'ma Zh. Eksp. Teor. Fiz. **72**, 825 (2000) [JETP Lett. **72**, 569 (2000)].